

University of Alberta
Department of Civil Engineering



Structural Engineering Report No. 190

ANALYSIS AND DESIGN OF
FABRICATED STEEL STRUCTURES
FOR FATIGUE:
A PRIMER FOR CIVIL ENGINEERS

by

G.L. KULAK

and

I.F.C. SMITH

July 1993

Analysis and Design of Fabricated Steel Structures for Fatigue:

A Primer for Civil Engineers

by

**Geoffrey L. Kulak
Department of Civil Engineering
University of Alberta
Edmonton, Canada**

and

**Ian F.C. Smith
ICOM – Steel Structures
Swiss Federal Institute of Technology
Lausanne, Switzerland**

©

July, 1993

ACKNOWLEDGMENTS

As indicated by the References, the authors have drawn from the work of others in the preparation of this material. Every effort has been made to properly acknowledge such contributions. However, if any oversights are noticed, please communicate these to the authors.

The contributions of Manfred Hirt, Professor of Steel Construction and Director of, ICOM, Swiss Federal Institute of Technology, Lausanne, and Professor John W. Fisher, Director of the Center for Advanced Technology for Large Structural Systems, Lehigh University, Bethlehem, Pennsylvania are gratefully recognised. Professor Hirt is the co-author of a principal source documents (Reference 1). The authors also thank Dr. Peter Kunz, ICOM, for his help with the preparation of Example 6.

Figure 5 is taken from Hirt, M.A. "Anwendung der Bruchmechanik für die Ermittlung des Ermüdungsverhaltens geschweisster Konstruktionen," *Bauingenieur*, 57 (1982), and is used with his permission. Figures 13, 14, and 15 are the results of studies directed by John Fisher. These figures are copyrighted by the Canadian Institute of Steel Construction and are used with permission.

TABLE OF CONTENTS

1. INTRODUCTION	1
2. BASIC FRACTURE MECHANICS CONCEPTS	2
2.1 How to Account for a Crack	2
2.2. Fracture Limit State	4
2.3 Fatigue Limit State	7
2.4 Fracture Mechanics used as a Qualitative Design Tool	10
3. FATIGUE STRENGTH ANALYSIS	14
3.1 Introduction.....	14
3.2 Sources of Flaws in Fabricated Steel Structures	16
3.3 Basis for Design Rules	18
3.4 Design Rules Given by Representative Specifications	21
3.5 Fracture Mechanics Analysis of Fatigue	25
4. FATIGUE ASSESSMENT PROCEDURES FOR VARIABLE STRESS RANGES... 30	
4.1 Cumulative Fatigue Damage	30
4.2 Analysis of Stress Histories.....	33
4.3 Fatigue Limits.....	39
5. INSPECTION AND REPAIR OF FATIGUE CRACKS.....	43
5.1 Identifying the Causes of Cracking.....	44
5.2 Taking Appropriate Measures.....	45

5.3 Avoiding Future Cracking Problems.....	47
6. SPECIAL TOPICS.....	48
6.1 Role of Residual Stress	48
6.2 Combined Stresses.....	54
6.3 Effect of Size on Fatigue Life.....	55
6.4 Environmental Effects.....	55
6.5 Fatigue Cracking from Out-of-Plane Effects.....	57
6.6 Quantitative Design Using Fracture Mechanics	62
REFERENCES	65

1. INTRODUCTION

Many failures of engineering structures can be attributed to the presence of pre-existing cracks or crack-like discontinuities. The usual approach in the engineering design and execution of structures is to avoid details that might be prone to cracking and then to inspect the structures for cracks both during fabrication and later in their life. However, it is inevitable that cracks or crack-like discontinuities will be present, and it is the responsibility of the engineer to consider the implication of these, both in terms of brittle fracture and in terms of fatigue.

The purpose of this Primer is to provide both the student and practicing engineer with enough background that they will be able to understand and use the design rules for fatigue strength that are now a standard part of every design code for steel structures. The approach that is taken is to establish the basis for the problem in terms of a fracture mechanics approach, that is, an analytical tool that will handle problems of either fracture or fatigue [1]. Attention is then directed specifically toward the issue of fatigue.

Standard models for the design of beams, columns, trusses, and other structural elements use conventional stress analyses and a strength of materials approach. Such an approach is appropriate for the identification of the internal forces that result from static loading acting under conditions of normal temperatures and the use of relatively tough steel. However, it cannot be expected to adequately evaluate the effects of cracks in structural elements.

The development of the fracture mechanics method of analysis is a tool that has become available relatively recently. Originally developed to explain the rupture of glass specimens [2], its introduction into the field of structural engineering probably started when it was used in the 1940's to help explain the catastrophic failure of welded ship hulls. At the present time it is most employed by mechanical engineers, where it is used to assess elements in spacecraft, robotics structures, turbine blades, pipelines, automotive parts, and many other such components. In this Primer, the basic concepts of the fracture mechanics approach are described in order to assist the reader in understanding the fatigue design rules and, for those who might need to design at higher levels of sophistication, to provide the basis for further reading and self-teaching in this area.

2. BASIC FRACTURE MECHANICS CONCEPTS

A summary of fracture mechanics concepts is given in this section. For simplicity, the discussion is limited to cases where the load is applied at a location remote from the crack locations and normal to the crack surfaces, a so-called Mode 1 situation (see Example 1). Excellent review articles provide more detailed information (for example, see Ref. [3–5]) and several reference books are available [6–9].

2.1 How to Account for a Crack

Five cases of a plate containing a crack are shown in Fig. 1. It requires no knowledge of fracture mechanics to appreciate that cases 1 to 5 are placed in order of increasing severity. Taking case 1 as the basis for comparison, the following important fracture mechanics parameters can be identified: (i) crack length (case 2); (ii) crack location (at edge of plate in case 3); (iii) effect of bending (case 4); (iv) presence of a stress concentration (case 5). Of course, the effect of any of these parameters in weakening the plate will depend on the actual circumstances. The effect can be significant, however. For instance, the effect of a sharp stress concentration in combination with a crack (case 5) could weaken a plate to less than one-half of its uncracked strength.

A magnified view of the area around a crack tip in an infinitely wide plate is shown in Fig. 2. This resembles closely the conditions of case 1 when the crack length is small compared with the plate width. When a

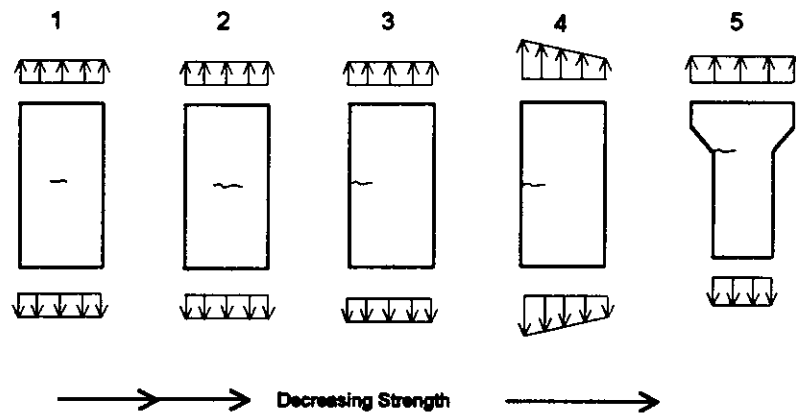


Figure 1 Five different cases of a plate containing a crack

remote stress, σ , is applied, the crack opens a certain distance, d , and the stress which this cross-sectional area would have carried is diverted to the uncracked area of the plate. This diversion creates a high concentration of stress in the vicinity of the crack tip. For an elastic material, theoretically this stress is infinite at the crack tip: in real materials, plastic zones are formed since the strain exceeds the ability of the material to behave elastically. This process—whereby an applied load (i) causes a crack to open, (ii) relieves crack surfaces of

stress, and (iii) creates crack-tip plastic straining—is the fundamental mechanism which weakens structures containing cracks or crack-like discontinuities.

A relatively simple description of the stress field near the crack tip can be obtained if plasticity is ignored. Using special stress functions, a solution containing the coordinates r and θ is developed. For the particular case of $\theta = 0$, that is, for the stress in the y -direction, the stress is:

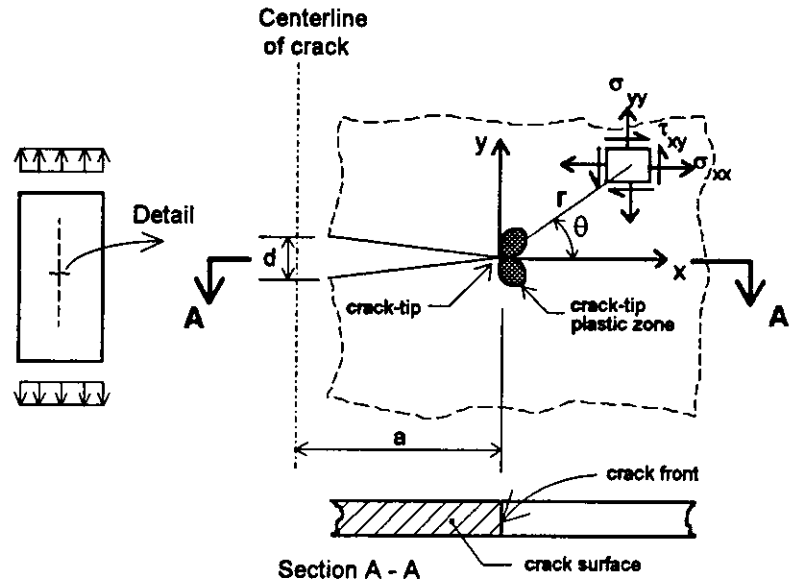


Figure 2 A crack in an infinitely wide plate

$$\sigma_{yy} = \frac{\sigma \sqrt{\pi a}}{\sqrt{2\pi r}} \quad (1)$$

provided that the crack length, a , is much larger than the distance from the crack tip, r . The numerator in Eq. (1) determines the gradient of the (theoretical) stresses as they rise to infinity when r approaches zero. This numerator is called the stress intensity factor, K . Thus:

$$K = \sigma \sqrt{\pi a} \quad (2)$$

The advantage of this model is that any combination of stress and crack length can be characterized by the single parameter K . Solutions are available for other particular geometrical configurations and loading conditions; these are summarized in handbooks [10] and compendiums [11]. However, many practical cases cannot be solved analytically. In such instances, the following expression is used to approximate K :

$$K = W Y \sigma \sqrt{\pi a} \quad (3)$$

where Y corrects for the presence of plate edges and curved-crack fronts and W corrects for non-uniform local stress fields caused by the presence of residual stresses, stress

concentrations, stress gradients due to thermal effect, and so on. Usually, such correction factors are determined using numerical methods.

Equation 1 is based on linear-elastic material behaviour and cannot account for the presence of plasticity at the crack tip. Furthermore, stress redistribution due to plasticity alters the stress field outside the crack-tip plastic zone. Nevertheless, if this zone is small, say less than 2% of the plate thickness, of the crack length, and of the uncracked ligament, then the stress intensity factor (K) approach is a satisfactory model.

The limitations are violated in many practical situations. For example, when stress concentrations cause localized plasticity an elastic-plastic analysis may be required. The most common analyses either use an expression for a variable named J, which is used to model the change in potential energy with respect to crack length, or use a parameter called the crack-tip opening displacement (CTOD). Further description of elastic-plastic analyses is available elsewhere [9] and ASTM has produced standards for determining them experimentally. (See, for example, Ref. [12]). Occasionally, an equivalent K is calculated [3]:

$$\frac{K^2}{E} = J = \sigma_y \text{ CTOD} \quad (4)$$

where E is Young's Modulus and σ_y is the effective yield strength. When plate dimensions are large enough to restrict behaviour to essentially two-dimensional straining (plane-strain conditions), the material constant, E, is replaced by $E / (1-\nu^2)$, where ν is Poisson's ratio.

A further restriction on K exists for small crack lengths, where all of the approaches explained above lose their validity. When the size of the crack or initial discontinuity is of the order of grain size, micro-structural properties such as grain orientation influence crack growth [13]. Microstructural fracture mechanics models may then become necessary. These models are not yet well defined, and no generally accepted design rules are available. For the usual situation, when the crack length is greater than about five grain diameters, the models that assume an isotropic continuum, i.e., those employing K or J, are sufficiently accurate.

2.2. Fracture Limit State

The analysis tools available will indicate that fracture occurs when the crack parameter (i.e. K or J) exceeds a critical value, commonly referred to as the fracture toughness. The designer should choose a steel with a fracture toughness level that is sufficiently high for the intended application. The fracture toughness depends upon such factors as material properties, service temperature, loading rate, plate thickness, and fabrication processes.

An accurate determination of the fracture toughness is complicated, especially for most structural engineering design. This is primarily due to the fact that, for most structural engineering designs, plane-strain conditions do not dominate; conditions of essentially two-dimensional stress (plane stress) have an influence, thereby disqualifying K as a model which characterizes combinations of stress and crack length. Elastic-plastic models are needed because the stress at fracture produces a plastic zone size that exceeds the limitations specified for the validity of K specified in Section 2.1.

Less sophisticated approaches are used for practical problems in structural engineering. The most widely used method for approximating the toughness quality of a steel is a procedure that was developed over 80 years ago, the Charpy impact test. Briefly, this method measures the energy absorbed by the rapid fracture of a small bar containing a machined notch. The bar is broken by a swinging pendulum and the absorbed energy is measured by the difference in swing height before and after fracture. The effect of temperature is examined by repeating the test using identical specimens that have been cooled to various temperatures. Several tests provide a relationship between absorbed energy and temperature for the steel under investigation—see Fig. 3 (a).

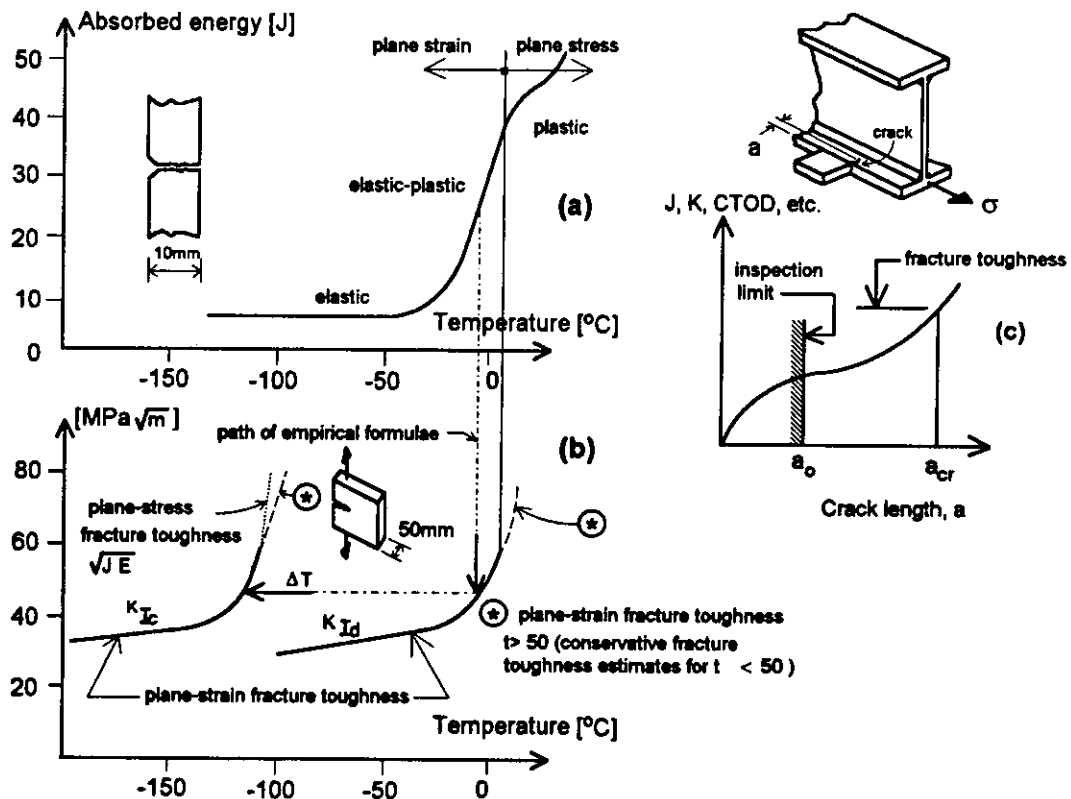


Figure 3 Basic considerations for a fracture assessment. (a) Typical results of Charpy-V impact tests; (b) Typical fracture-toughness results; (c) Conversion to critical crack length, a_{cr}

The Charpy test, and many other similar procedures [9] provide only qualitative information because stress and crack length values cannot be assessed directly. However, correlations with fracture mechanics models are available for certain situations [8]. For example, Charpy impact data in the lower region of the curve in Fig. 3(a) can be converted into dynamic plane-strain fracture toughness values, K_{I_d} , using an empirical formula.¹ If required, the K_{I_d} values can be converted to static plane-strain fracture toughness values, K_{I_c} . Conventionally, this is done by means of a horizontal temperature shift to the left, ΔT , as shown in Fig. 3(b), although a designer is really interested in the vertical change at a given temperature. Additional curves between K_{I_d} and K_{I_c} , which correspond to intermediate loading rates, can also be defined. In general, such correlations are valid only for steels of low to medium strength. Moreover, the toughness value where conditions change from plane strain to plane stress depends upon the yield strength and the thickness of the element. The location of this change cannot be correlated to Charpy results.

At a given temperature, a given material will always exhibit higher fracture toughness for plane-stress conditions than for plane-strain conditions in the elastic-plastic region. Therefore, K_{I_c} and K_{I_d} are conservative first estimates of the fracture toughness. Elastic-plastic analyses, which result in less conservatism, can be used when the design problem justifies increased complexity of work. A typical trend (in terms of J) is illustrated schematically by the dashed line in Fig. 3(b).

A critical crack length, a_{cr} , may be approximated by introducing the fracture toughness at the minimum service temperature and the maximum possible stress, σ , in Eq. 3—see Fig. 3(c). Fracture will not occur if the maximum size of the crack or crack-like discontinuity, a , is less than a_{cr} . Often, inspection technology influences this verification: a_{cr} is compared with the minimum verifiable crack length, a_0 . The engineer should ensure that the design configuration and the inspection equipment and procedures permit reliable detection of crack lengths less than a_{cr} .

The likelihood of fracture shortly after erection is not high in most modern structures. Some problems may arise when severe weld discontinuities are present or when very thick plates are used or when the structure is in a very cold environment, but such situations are not common. Rational designs which employ high-strength fine-grained steels and which use modern fabrication techniques should provide high toughness and, consequently, large critical crack lengths, a_{cr} . At the same time, careful assembly and improvements in the technology of

¹The subscripts used here for K are explained in Example 1.

non-destructive inspection are reducing the minimum verifiable crack length, a_0 . As a result, the greatest risks of fracture in modern steel structures arise when sub-critical crack growth due to fatigue, corrosion, stress corrosion, etc. is possible. Predicting the occurrence of the fracture limit state is becoming more dependent upon the correct choice of the sub-critical crack-growth model than upon an accurate estimate of the fracture toughness of the detail. Crack growth due to fatigue is discussed in the next section.

2.3 Fatigue Limit State

Fatigue is the initiation and propagation of microscopic cracks into macro cracks by the repeated application of stresses. (As we will see later, the initiation portion of fatigue life is essentially zero for fabricated steel structures). In civil engineering practice, fatigue cracking occurs most often in structures such as bridges, cranes, towers, and any such structure which is subjected to repeated loading. Although today's steel structures use higher-toughness materials than was common in the past, and are thus more fracture-resistant than ever before, many structural elements remain susceptible to fatigue crack growth. Consequently, if the fracture limit state is reached, it is often the result of fatigue crack growth after many years of trouble-free service. Such an occurrence is covered by the definition of the fatigue limit state.

In addition to higher-toughness properties, development of low-alloy and fine-grain microstructures have increased the yield strengths of the steels used for construction. Consequently, higher service stresses have been allowed in recently built structures. Furthermore, welding is now used more often than formerly, and, as will be seen, this method of fastening leads to a lower fatigue life than would apply if the connection was made using rivets or bolts. Generally speaking, then, modern structures are more susceptible to fatigue cracking than were older structures. Furthermore, the number of old structures, for example railway bridges, that have exceeded their design fatigue life is growing exponentially. The combined effect of these trends is increasing the importance of fatigue strength evaluation.

All elements of a fabricated steel structure contain metallurgical or fabrication-related discontinuities and most also include severe stress concentrators such as weld toes. Consequently, fatigue failure is often the result of slow crack growth from an existing discontinuity at a stress concentration. This growth can even begin before the structure is put into service (the result of transportation of a girder, for example). A description of the fatigue crack growth phenomenon can be made on the basis of the fracture mechanics model described in Section 2.

The stress intensity factor K can be modified to represent fatigue crack growth by adapting Eq. 3 to account for repeated loading. For a constant stress range, $\Delta\sigma$ ($=\sigma_{\max} - \sigma_{\min}$), Eq. 3 becomes

$$\Delta K = W Y \Delta\sigma \sqrt{\pi a} \quad (5)$$

Equation 5 is related empirically to the crack-growth rate, da/dN , which is obtained from the slope of the curve of crack-growth measurements—see Fig. 4(a). This slope is used as the ordinate in a plot of this parameter against ΔK , using a double logarithmic representation—see Fig. 4(b). The values of ΔK are calculated using Eq. 5 for particular magnitudes of crack length, a . At very low growth rates, the curve for crack growth (in steel) becomes vertical, indicating a crack-growth threshold at ΔK_{th} , the threshold stress intensity factor. At higher values of ΔK , the curve straightens to a near-constant slope, and it becomes vertical again when the fracture toughness is approached at the maximum stress in the cycle.

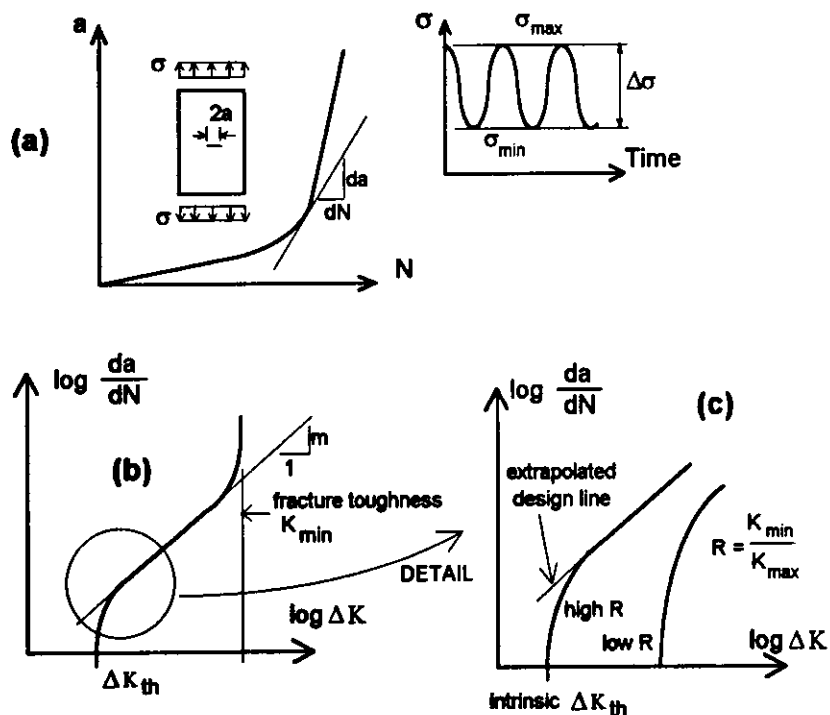


Figure 4 The stress-intensity factor and fatigue crack growth. (a) Crack length vs. number of cycles; (b) Crack growth rate vs. stress intensity factor range; (c) Magnification of the lower portion of the curve in (b)

Material properties, stress level, and environment have greater influence in the end (vertical) portions of the curve than in the middle. In this center portion, which is of considerable engineering interest, the Paris law is useful [14]:

$$\frac{da}{dN} = A \Delta K^m \quad (6)$$

where A and m are constants that are determined by means of regression analysis of test data. These constants are reliable when similar materials, loadings, and environments are compared. (The constants show up directly in the design specifications, as will be seen in Section 3.5) Also, the regression analysis is dependent upon the domain of crack growth rates considered since the center portion of the curve in Fig. 4(b) is not perfectly straight.

Many structural applications involve repeated loading of over one million cycles: this requires a precise knowledge of slow crack growth rates near ΔK_{th} —see Fig. 4(c). Conservative assessments result when Eq. 6 is extrapolated into this region. The error resulting from the extrapolation is dependent upon the magnitude of the stress ratio, $R = \sigma_{max}/\sigma_{min}$. This ratio is often used to examine the effects of mean stress on crack growth.

When ΔK is much larger than ΔK_{th} , Eq. 6 can be integrated to calculate the crack propagation fatigue life, N :

$$N = \frac{1}{A} \int_{a_i}^{a_f} \frac{1}{\Delta K^m} da \quad (7)$$

where a_i and a_f are the initial and final crack lengths. These integration limits may take the values a_0 and a_{cr} , respectively, as defined in Section 2.2.

Variable amplitude loading may be assessed in a cycle-by-cycle integration. This integration may follow a procedure comparable to the calculation of the equivalent constant amplitude stress range which is recommended in some design codes [15,16]. This is discussed in Section 4.2.

It was pointed out in Section 2.2 that small crack sizes and excessive plasticity may invalidate models which employ the stress intensity factor. This is equally true for fatigue applications: non-conservative calculations may result if so-called short crack behaviour occurs [17]. Fortunately, such situations are less common when assessing the fatigue limit state. Usually, the stress intensity factor remains a useful characterizing parameter for conditions of fatigue crack growth since discontinuities are large and a high percentage of crack growth occurs under conditions where K is valid. Moreover, structural engineering applications have particular characteristics that reduce the occurrence of this anomalous behaviour.

2.4 Fracture Mechanics used as a Qualitative Design Tool

Engineering designers rarely use fracture mechanics as a design tool. Older concepts, such as Charpy energy values for fracture toughness requirements and stress range models for fatigue assessments (see Section 3.4), are the most practical tools for evaluating many structures. Nevertheless, the concepts of fracture mechanics enable the designer to increase his qualitative understanding of structures containing crack-like discontinuities. Because more parameters are explicit in fracture mechanics analyses, designers can identify more easily those parameters that influence the strength of the structure. Some examples, covering the importance of discontinuities, parametric studies, and crack propagation behaviour, are presented below. Guidelines for simple linear-elastic fracture mechanics models sufficient for most structural engineering designs are available in some design codes [15] and one illustration of the application of fracture mechanics analysis is given in Section 3.5.

The size of the discontinuity clearly influences the resistance of an element to fracture. For example, two trends are illustrated by the curves in Fig. 5(a). First, increasing the applied stress causes a decrease of the critical defect size. Second, an embedded discontinuity (such as an inclusion) is less serious than a surface discontinuity (such as a weld undercut). Fracture mechanics analysis clarifies the importance of discontinuities in fracture assessments. This has resulted in an increased emphasis on quality assurance guidelines [18] and on detail designs that have small discontinuities.

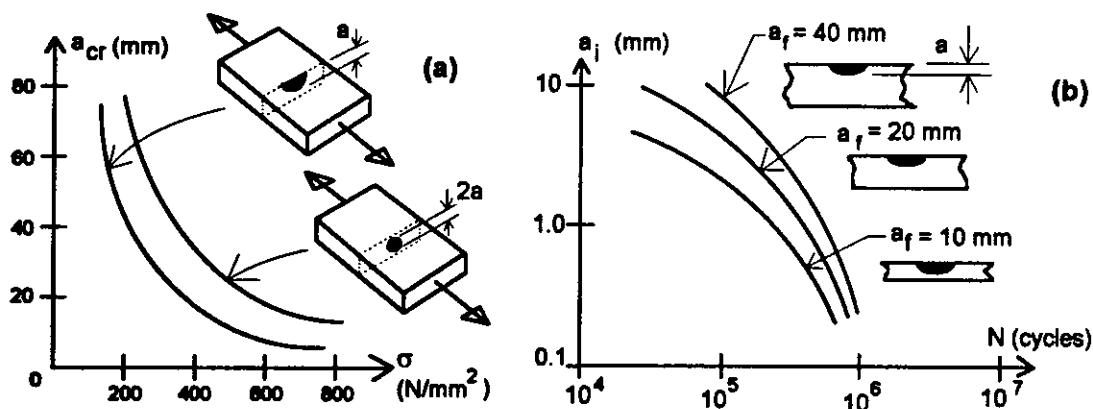


Figure 5 Examples of studies that examined the significance of discontinuities (a) Critical crack size vs. applied stress; (b) Effect of initial and final crack size on fatigue life

The effect of discontinuities is equally important when assessing the fatigue limit state. The integral in Eq. 7 has the limits a_i and a_f . Small variations in the magnitude of the final

crack size, a_f , may not significantly alter the resulting fatigue life. The initial crack size is far more important than the final crack size—see Fig. 5(b).

Fracture mechanics analysis facilitates recognition that, when the end plate shown in Fig. 6 is welded to the beam, the areas which are not welded become built-in cracks. Groove welding may not always be able to penetrate completely into the unwelded zone. Cope holes, which give better access to this area and thus eliminate unwelded portions, increase the strength of these details. Design guidelines already recognize that flange fillet welds will result in an even lower fatigue strength than that of these details because the resulting unwelded areas (cracks) will be even larger than the area shown in Fig. 6.

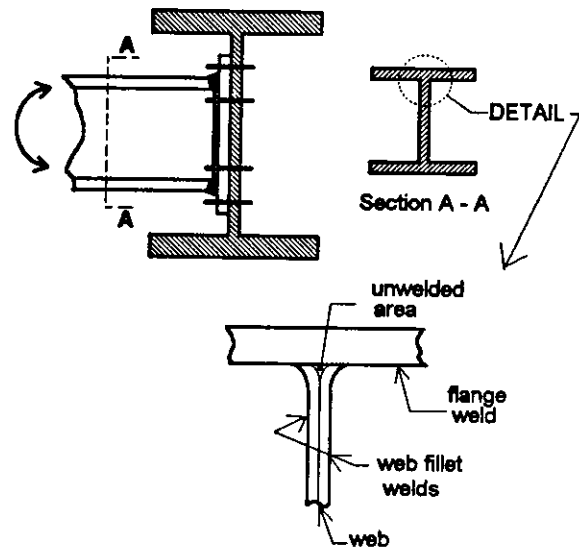


Figure 6 Unwelded areas can become built-in cracks

Design specifications cannot provide fatigue strength information for every possible structural shape and detail. However, it is usually possible to identify in the specification details that are similar to the one under consideration. A parametric study using fracture mechanics can be used to determine whether the identification is correct or, alternatively, what extra effects should be considered. For example, about ten years ago fracture mechanics analyses showed that increasing the plate thicknesses in connections employing transverse fillet welds (cruciform joints) reduced the fatigue life [19]. After testing verified this prediction [20], new specification provisions were introduced [21]. (Section 6.3 discusses thickness effects in more detail.) Similarly, a fracture mechanics study revealed that an increase in fatigue life can be expected when plate thickness is increased in the case of longitudinal fillet-welded attachments [22].

A fatigue crack that starts at the surface of the material initially propagates very slowly into the plate thickness. The stress concentration, modeled by the parameter W in Eq. 5, affects the crack growth rate. Connections classified by specifications as falling into different fatigue strength categories [15] may have different crack propagation characteristics for the same fatigue life—see Fig. 7.

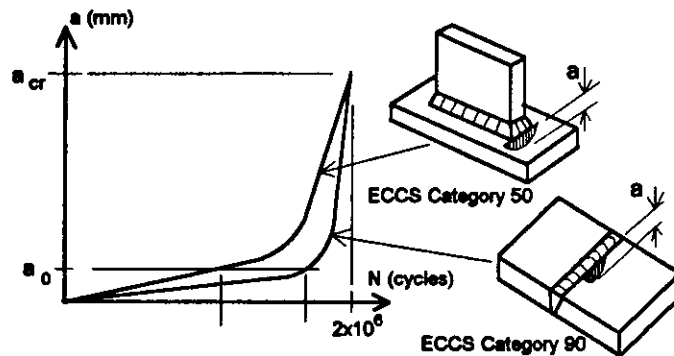


Figure 7 Comparison of fatigue crack growth behaviour for two different details having the same fatigue life

In this example (Fig. 7), the detail with lower-severity stress concentration (groove-welded plate) consumes a greater percentage of its total fatigue life during the propagation of a crack to a size a_0 than does the detail with a higher-severity stress concentration (attachment detail). This means that a crack of a given size may be identified earlier at the attachment than at the groove weld. Other factors such as differences in inspection feasibility influence the exact timing of crack identification. Nevertheless, such crack growth behaviour should be considered when establishing inspection intervals.

Example 1

Crack opening modes are shown in Fig. 8. In structural engineering applications, Mode I will almost always be the applicable case. In order to distinguish among the various possible cases, the stress intensity factor K introduced in Section 2.1 is subscripted, e.g., K_I would be used for a Mode I case. The value of the stress intensity factor at which brittle fracture will occur is designated as K_{Ic} or as K_{Id} , depending upon whether the loading is essentially static (K_{Ic}) or dynamic (K_{Id}).

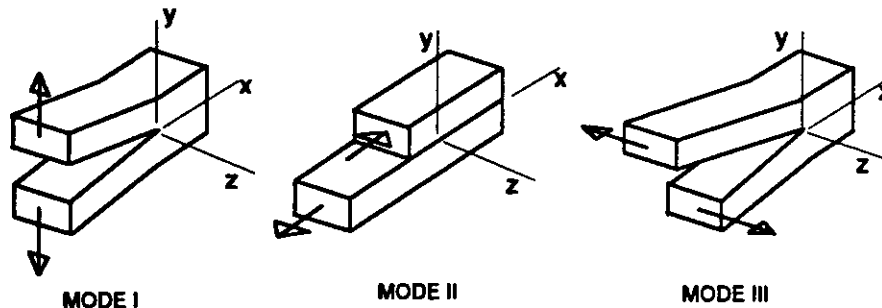


Figure 8 Basic modes of loading involving different crack surface displacements

Published solutions for the expressions for the stress intensity factor are available for a wide variety of cases [10]. Several common cases are shown in Fig. 9.

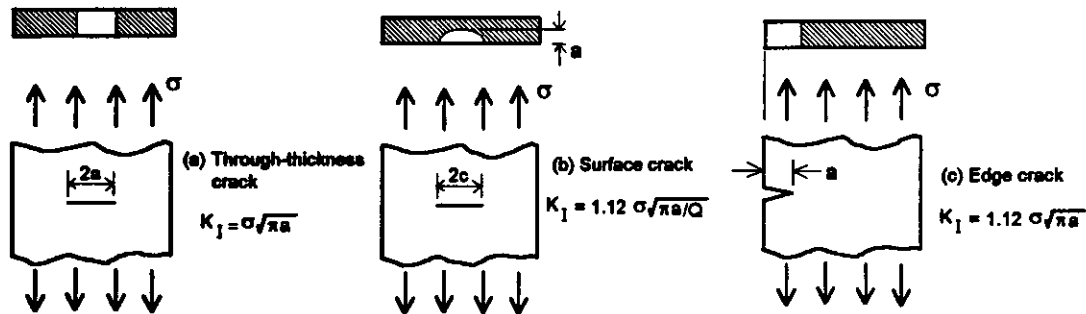


Figure 9 K_I values for various crack geometries

Consider the element shown in Fig. 10, where a centrally located through-thickness crack is present in a plate that is loaded by a uniform tensile stress.

Given: $\sigma_y = 550 \text{ MPa}$

$K_{Ic} = 66 \text{ MPa m}^{1/2}$ (This information is provided by the supplier of the material and is related to the intended service temperature, loading rate, and the particular plate thickness.)

Design stress = 140 MPa

Question: (a) What is the flaw size at which brittle fracture might be expected?

Solution: It is given that the value of the critical stress intensity factor is $K_{Ic} = 66 \text{ MPa m}^{1/2}$. From Fig. 9, the general expression for the stress intensity factor is $K_{Ic} = \sigma\sqrt{\pi a}$. It is simply a matter of examining the situation $K_I \rightarrow K_{Ic}$, or

$$\sigma\sqrt{\pi}\sqrt{a} = 66 \text{ MPa}\sqrt{m}$$

$$\text{Using } \sigma = 140 \text{ MPa and solving, } \sqrt{a} = 0.27\sqrt{m}$$

$$a = 0.071\text{m} = 71\text{mm}$$

Thus, if the flaw size reaches $2a = 142 \text{ mm}$, failure by brittle fracture can occur.

Question: (b) If the design stress is increased to 310 MPa, what is the tolerable flaw size now?

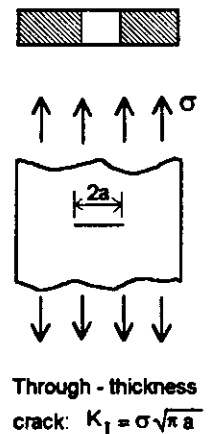


Figure 10

Solution: $\sigma\sqrt{\pi}\sqrt{a} = 66 \text{ MPa}\sqrt{\text{m}}$

$$310 \text{ MPa} \sqrt{\pi}\sqrt{a} = 66 \text{ MPa}\sqrt{\text{m}}$$

Solving, $2a = \text{flaw size} = 29 \text{ mm}$.

Question: (c) Residual stress due to welding is present and it is estimated that the total stress (design stress + residual stress) is 500 MPa. What is the tolerable flaw size now?

Solution: $\sigma\sqrt{\pi}\sqrt{a} = 66 \text{ MPa}\sqrt{\text{m}}$

$$500 \text{ MPa} \sqrt{\pi}\sqrt{a} = 66 \text{ MPa}\sqrt{\text{m}}$$

Solving, $2a = \text{flaw size} = 11 \text{ mm}$.

Comment: Often, it is not possible to superimpose stresses due to residual stresses because—

1. The distribution of residual stress is different from the applied stress. (Recall that the expression in Fig. 9 is valid only for a uniform, remote stress);
2. There is a stress concentration present. This requires that a correction factor for K be used on the applied loads, but not for the residual stresses;
3. There is a possibility of residual stress relaxation with crack growth. In such cases, the value of K for residual stresses should be calculated separately and then added to the K for the applied loads. Thus, superposition is applied at the level of K. Note that K was determined to be the parameter that characterizes cracks because use of other parameters, e.g., σ , can lead to erroneous results.

3. FATIGUE STRENGTH ANALYSIS

3.1 Introduction

The approach taken by modern-day specifications for the design of fabricated steel structures is based primarily by the work done by Gurney in Great Britain [23] and by Fisher in the USA [24–26], which took place in the late 1960's and early 1970's. Although many other researchers have contributed to our understanding of the problem, both before and after the work cited, it was perhaps these persons (and their co-workers) who more than others identified the influence that residual stress plays in determining fatigue life and emphasized the

necessity to acknowledge that fabricated steel structures always contains cracks or crack-like discontinuities.

Fatigue has been defined as the initiation and propagation of microscopic cracks into macro cracks by the repeated application of stress. In terms of the fracture mechanics model described in Section 2, an initial crack grows a small amount in size each time a load is applied. A good explanation of the crack growth mechanism has been provided by Broek [27]. Growth occurs at the crack front, which is initially sharp. Even at relatively low loads, there will be a high concentration of stress at the sharp front, and plastic deformation (slip on atomic planes) therefore occurs at the crack front. Continued slip results in a blunted crack tip, and the crack grows a minute amount during this process. Upon unloading, not necessarily to zero, the crack tip again becomes sharp. The process is repeated during each load cycle.

Figure 11 shows the fracture surfaces of a member which has an I-shaped cross-section. The web of the member, which was $3/8$ inch (10 mm) thick, was fillet-welded to $1/2$ inch (13 mm) thick flange plates. (The full thickness of the flange is not shown in Fig. 11). The profiles of the fillet welds are generally satisfactory and the flow lines of the weld show good penetration of the base metal. In this

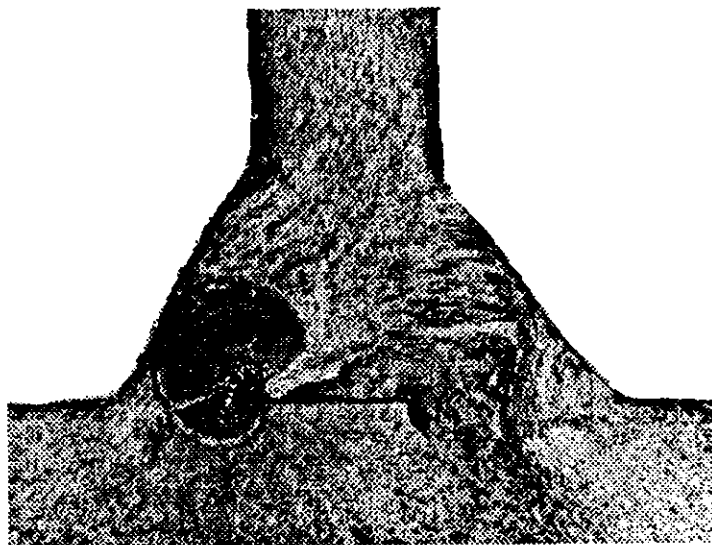


Figure 11 Fracture surface of I-shaped member

illustration, an internal flaw in the left-hand fillet weld grew under the repeated application of stress until the crack penetrated the outside surface of the weld. Since this was a laboratory specimen, at this point the beam was deliberately overloaded so that the remaining cross-section fractured and could be exposed.

In the case illustrated in Fig. 11, the crack front eventually reached the exterior surface of the weld. Experience in the laboratory shows that as much as 80% of the maximum fatigue cycles can have been consumed by the time a fatigue crack emanating from an internal flaw reaches the surface and can be observed in the laboratory.

If the test which produced the specimen shown in Fig. 11 had not been terminated in the particular manner described, failure could have occurred in one of two ways. One possibility is that the fatigue crack grows to such an extent that the loss of cross-section means that the load simply cannot be carried any longer by the uncracked portion of the beam. In this case, failure occurs by yielding of the remaining material, or, exceptionally, by instability if the crack growth produces a grossly unsymmetrical cross-section. The other way that the beam can fail is by brittle fracture. As discussed in Section 2.3, growth of a crack by fatigue can lead to brittle fracture if the crack reaches a critical size according to the particular conditions of material toughness, temperature, and loading rate.

3.2 Sources of Flaws in Fabricated Steel Structures

The kinds of flaws that can occur in a fillet-welded detail are shown in Figure 12. These include partial penetration and lack of fusion, porosity and inclusions (the fatigue crack shown in Fig. 11 started at a non-metallic inclusion), undercut or micro flaws at the weld toe, and cracking or inclusions around a weld repair or at start-stop locations or at arc strikes. Although the fabricator of the structure and those responsible for the fabrication inspection will attempt to minimize these defects, it is neither practical nor economically possible to eliminate them in all cases.

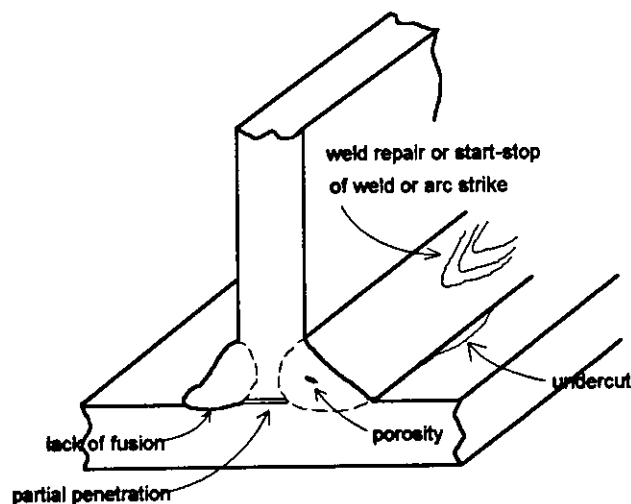


Figure 12 Flaws in a fillet-welded detail

In some cases, a "defect" is an expected result of the type of fabrication process and has no effect on the life of the member. For instance, the partial penetration shown in Fig. 12 (which is also seen in the welded beam of Fig. 11) is a natural consequence of the fillet-welded connection: it is not expected that the two fillet welds will merge in the central region of the connection. Furthermore, since the crack represented by the lack of penetration is parallel to the direction of the (bending) stress field, a so-called Mode II crack (see Fig. 8), the crack will not open up under the application of stress and failure by fatigue is unlikely. Consider a detail involving mechanical fasteners—an I-shaped beam with a cover plate fastened to the beam flange with bolts. The region between bolt lines is a "flaw" or "crack", but, since the discontinuity is parallel to the stress field, the "crack" does not grow and therefore its presence does not affect the fatigue strength of the member.

The flaws that exist in all fabricated steel structures are a consequence of the manufacturing process of the steel itself and the normal fabrication processes. Flaws in rolled shapes arise from surface and edge imperfections, irregularities in mill scale, laminations, seams, inclusions, etc., and from mechanical notches due to handling, straightening, cutting, shearing, etc. In a rolled shape, crack growth can start from one of these sources. Comparatively, the "unaltered" rolled shape presents the most favourable fatigue life situation. However, there are not many practical cases in which a rolled shape does not have some kind of attachment, connection, or some other kind of alteration.

Mechanical details, in which holes are drilled or punched and forces are transferred by means of rivets or bolts, present a somewhat more severe fatigue life situation. Drilled or sub-punched and reamed holes give some reduction in fatigue life as compared with an unaltered member, but the difference usually is not very great. If preloaded high-strength bolts are used, the disturbing effect of the hole is largely masked by the presence of the high local compressive stresses introduced by the bolt. Punched holes give a greater reduction in fatigue life than do drilled or sub-punched and reamed holes because of imperfections at the hole edge arising from the punching process. In this case, the crack usually starts at the edge of the hole.

Broadly speaking, any mechanical detail has a better fatigue life than does its equivalent welded detail. The types of flaws introduced when welding is used have already been discussed. In addition to the fact that more flaws will be present when welding is used, inspection for defects is more difficult than is the case for mechanically fastened details. Likewise, repair of welded details is often difficult. Prohibiting the use of welded details in fatigue situations is not a practical option, however.

The task of the structural engineer is to be able to proportion those structural members that have a potential for failure by fatigue crack growth so that they have a sufficiently long life as compared with the design life of the structure. As we will see, this will be done in the environment that some probability of failure must be accepted: in real terms, there is no structure that can be designed for zero probability of failure. The design will be carried out in the expectation that flaws will be present initially in all fabricated steel structures and that all such members will contain residual stresses of relatively high magnitude. A concomitant feature is that in the design process it is possible to identify the size of flaws that are permissible and then to use this information as the basis for both initial inspection of the structure as well as on-going inspection. This latter feature is not yet well-developed in design

specifications, and the usual procedure is to accept as permissible flaw sizes consistent with the specifications that accompany the fabrication processes, e.g., the welding specifications.

3.3. Basis for Design Rules

To those working in the research area, it was evident that the features that needed to be examined included the yield strength of the steel (reflected by the grade of steel), the number of cycles of load to which the member was subjected, some aspect of the stress itself, and the stress concentration present.

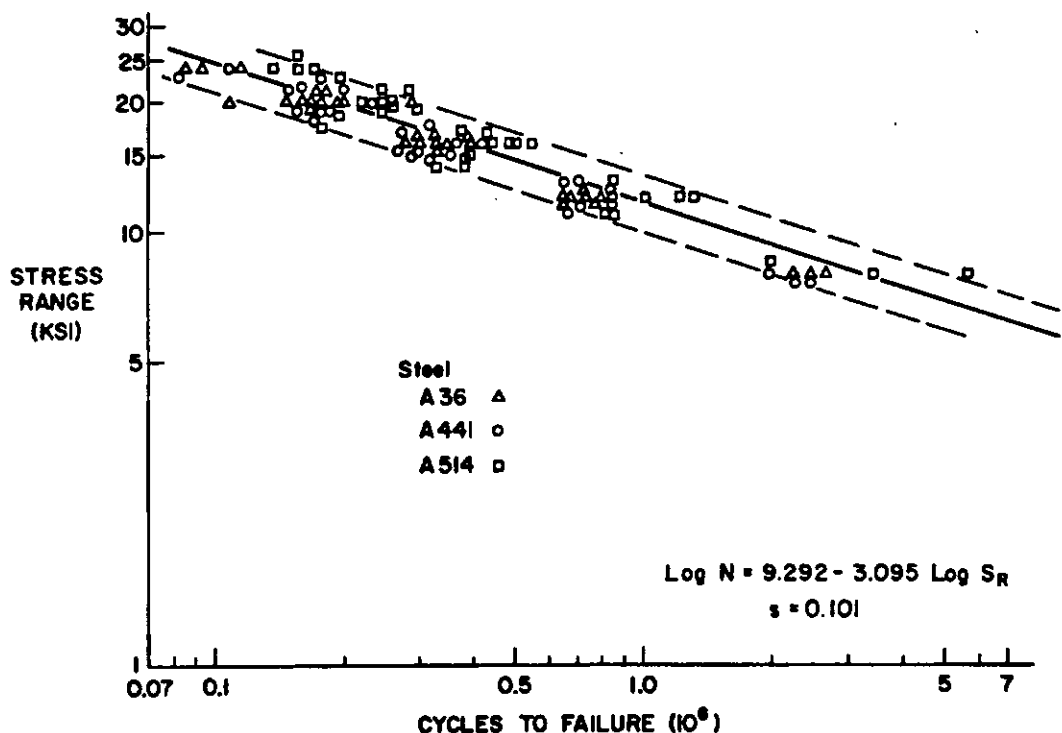


Figure 13 Effect of grade of steel on fatigue life of beams with transversely end-welded cover plates

Figure 13 shows a plot of the stress feature versus the number of cycles to failure for a given detail (beams with transversely end-welded cover plates) for three different grades of steel. These particular steels represent the spectrum of steel strengths used at the present time—from 36 to 100 ksi (250 to 690 MPa). Given that a certain amount of scatter is always present in results of this kind, it is evident that the yield strength of the steel does not have a significant influence on the results. Other information contained in this figure is significant and is typical of all fatigue strength tests results. First, the data plot as a straight line in this log-log representation. Secondly, the data are contained within a reasonably well-defined band about the mean. In Fig. 13, the parallel lines plotted two standard deviations away from the mean

line (measured relative to the horizontal axis) contain most of the test results. The degree of scatter in the results will have to be considered when a choice is made for a design life line. Customarily, this choice is made for the designer by the specification itself.

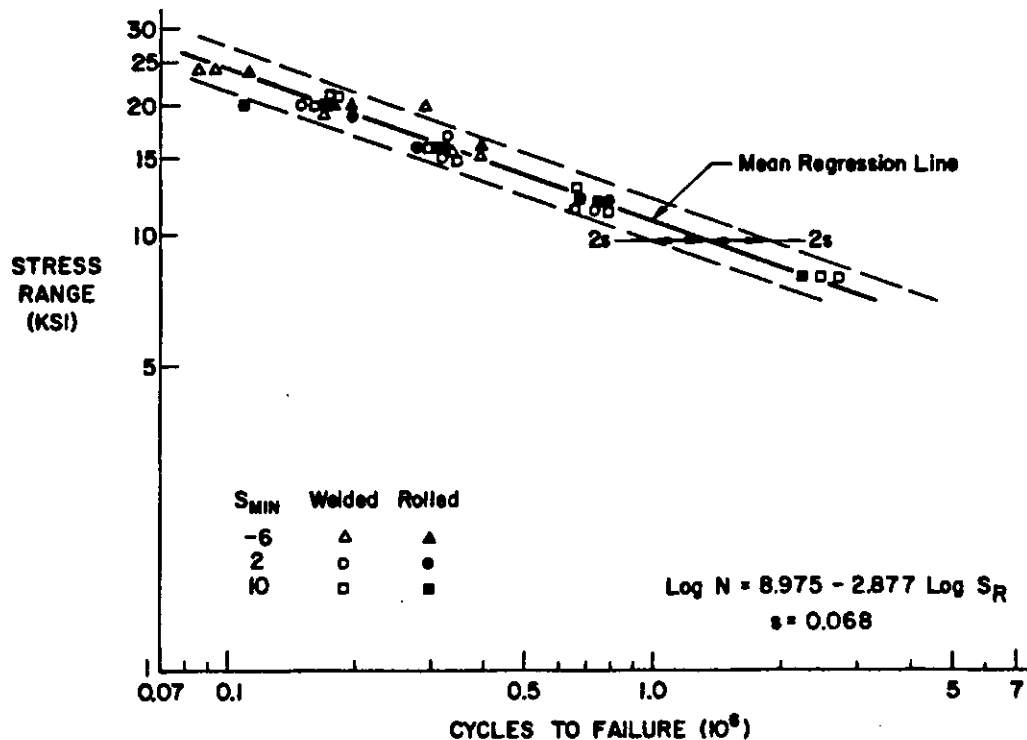


Figure 14 Effect of stress range and minimum stress on fatigue life for welded end of coverplated beams

The way the stress feature should be represented is examined in the data contained in Fig. 14. Considering again the end-welded cover-plated beam (both as-rolled and three-plate welded beams are represented in Fig. 14, however), the effect of stress is introduced as the stress range, that is, the algebraic difference between the maximum stress and the minimum stress at the critical location ($\Delta\sigma_r = \sigma_{max} - \sigma_{min}$). The tests represented in Fig. 14 were done at values of minimum stress (σ_{min}) equal to -6 ksi, 2 ksi, and 10 ksi, and, of course, a spectrum of stress range. Examine, for example, the data plotted for the stress range of 20 ksi. For this stress range, this means that the maximum stresses had to have been 14 ksi, 22 ksi, and 30 ksi, respectively, for the three values of minimum stress. It is obvious that the data are closely grouped and that the minimum stress *per se* does not influence the results. As will be seen in Section 6.1, it is the presence of high levels of residual stress that dictates that stress range is the controlling stress parameter for a description of fatigue life, rather than maximum stress, minimum stress, or stress ratio (i.e., $\sigma_{max}/\sigma_{min}$).

In accordance with the ideas developed in Section 2, Basic Fracture Mechanics Concepts, it would be expected that stress intensity (K) should be represented in the fatigue life evaluation. For the usual level of design, this is not a practical solution, however, and a more expedient approach is taken. This is simply to arrange standard structural details into categories relative to their expected fatigue life. For example, illustrated in Fig. 15 are the fatigue life representations for two different categories—beams which have cover plates that include a weld across their ends and beams made up of three plates welded together, such as the beam illustrated by Fig. 11. Clearly, if the designer had one of the two types of members shown in Fig. 15, presumably he now would be able to design those members for fatigue life.

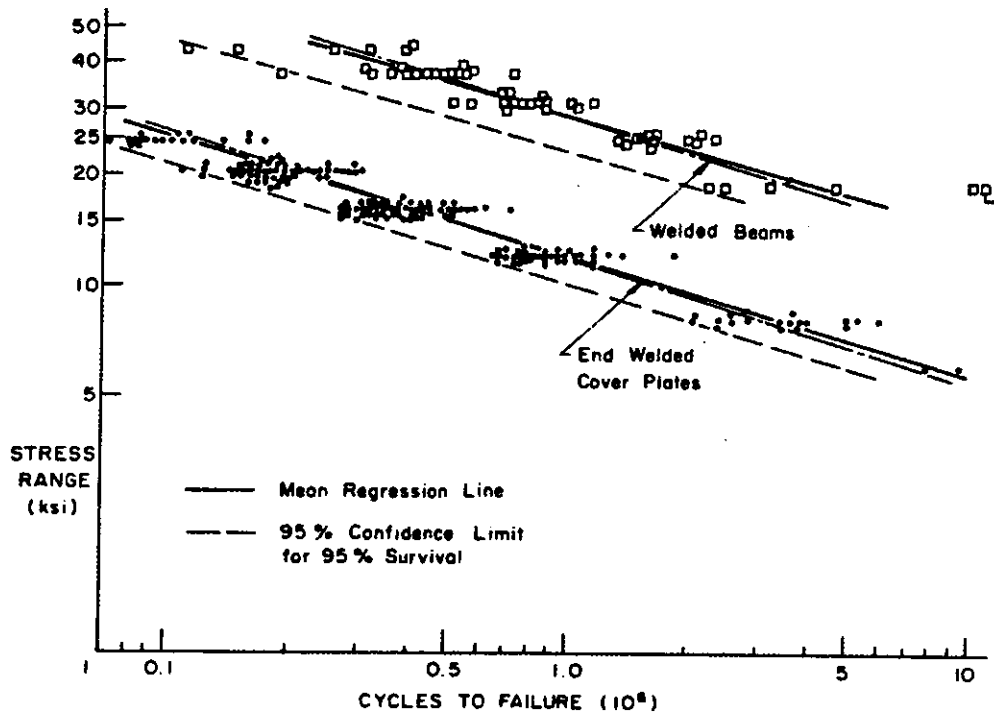


Figure 15 Fatigue strength of welded and coverplated beams

In summary, the fatigue life of a fabricated steel structure can be associated principally with three factors. These are:

1. the number of cycles of loading to which the member is subjected;
2. the type of detail under examination;
3. the stress range at the location of the detail.

The stress range to be calculated is simply that corresponding to the nominal stress at the location of the detail. This is valid because selection of the detail itself implies inclusion of the stress concentration for that detail.

3.4 Design Rules Given by Representative Specifications

Typical rules used for the fatigue strength design of fabricated steel structures will be represented by one European specification and one North American specification. The former is a document of the European Convention for Constructional Steelwork (ECCS) [15]. It is used as the basis for the fatigue strength specifications of the International Standards Organization, Eurocode, and the Swiss national standard, for example. The North American document is that published by the American Association for State Highway and Transportation Officials (AASHTO) [28]. It is used extensively in the United States. Specifications used in Canada [29,30] are similar to the AASHTO specification. Although the ECCS and AASHTO documents differ in some details, they are based on the same philosophical approach to the problem.

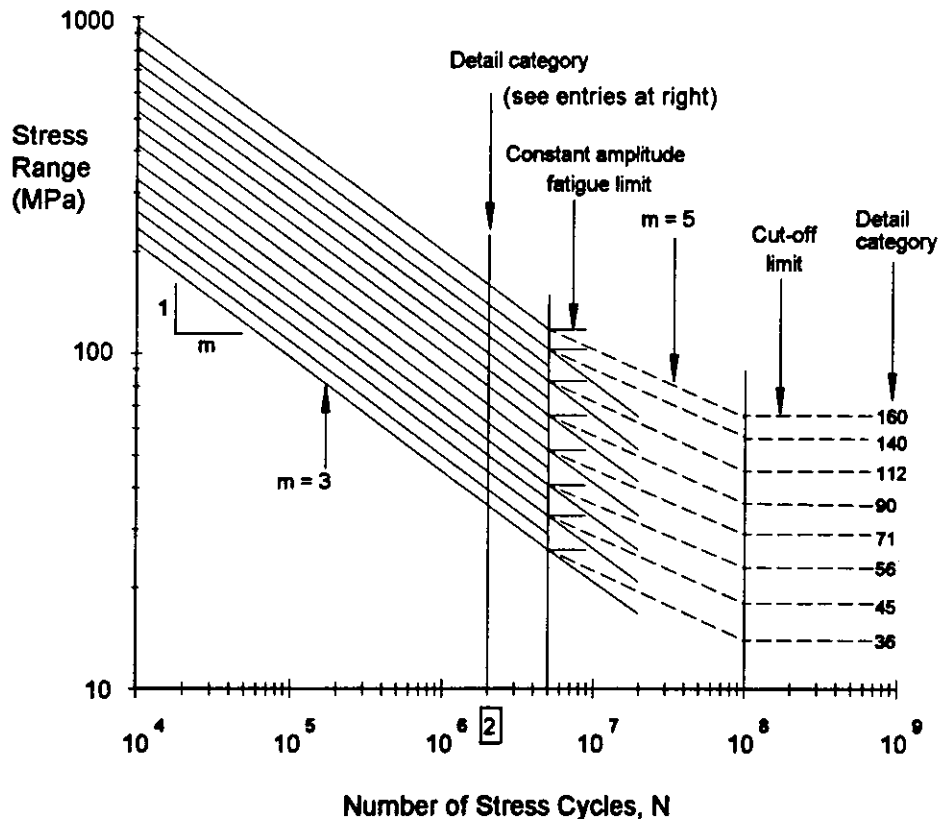


Figure 16 Fatigue life rules according to the ECCS specification [15]

Figure 16 shows the fatigue life curves given in the ECCS rules. The plot shows stress range on the vertical axis and number of cycles on the horizontal axis for fourteen different detail categories. Both axes are logarithmic representations. For convenience, these categories are identified by the numerical value of the permissible stress range of that category at 2×10^6

cycles. (Because of limited space, in Fig. 16 the detail categories are shown by the extension of each line, on the right hand side of the graph. Also, it is not possible to list every detail category. For example, Detail Category 125, not listed, lies between Categories 140 and 112.) Over most of the range, each category is a sloping straight line with a slope constant m equal to 3. Beyond 5×10^6 cycles, the slope constant can either be zero, 3, or 5, and this feature will be discussed subsequently. Another change occurs for number of cycles greater than 100×10^6 cycles, and this feature will also be discussed later.

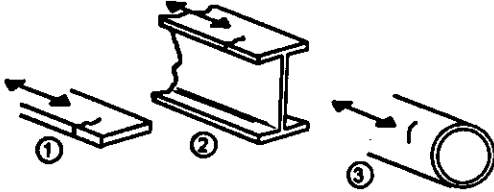

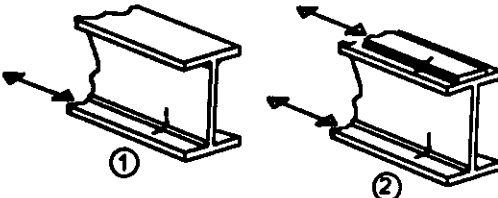
Detail Category	Constructional Detail	Description
160		<u>Rolled and extruded products</u> 1. Plates, flats 2. Rolled sections 3. Seamless tubes Requirements for details 1 to 3: Sharp edges, surface and rolling flaws to be improved by grinding.
140		<u>Sheared or gas-cut plates</u> 4. Machine gas-cut or sheared material subsequently dressed to remove all visible signs of edge discontinuities.
125		<u>Continuous longitudinal welds</u> 1. Automatic butt welds carried out from both sides. Category 140 may be used if the welds are shown to be free of detectable discontinuities 2. Automatic fillet welds. Cover plate ends should be verified, see ... Requirements for details 1 and 2: no stop-start positions.

Figure 17 Example of fatigue categories used in the ECCS Specification [15]

Figure 16 must be used in conjunction with the type of information shown in Fig. 17, where a few of the relatively large number of typical construction details classified by the specification are shown. Application of the information is straightforward. For example, suppose a designer proposes to use a beam made by joining three plates using fillet welds, such as was illustrated in Fig. 11. According to Fig. 17, this is detail category 125. If the number of cycles to which the beam will be subjected is, say, 2×10^6 , then the permissible range of stress for this detail is 125 MPa. If the number of cycles is, say, 300 000, then the permissible range of stress is slightly more than 200 MPa. (Working out the equation of the

line for this detail category, the "exact" value of the permissible stress range at 300 000 cycles is 235 MPa. As will be seen later, both the ECCS and AASHTO specifications allow the rapid calculation of the permissible stress range corresponding to a given number of cycles.)

The fatigue strength curves presented in the ECCS specification are those corresponding to the mean life of a detail, usually as obtained by physical testing, shifted horizontally to the left by two standard deviations. For reasonably large numbers of test data, the corresponding confidence limit is generally estimated to be approximately 95%. If a more sophisticated description of the safety of a member is desired, an appendix to the specification provides information as to how to incorporate uncertainties respecting both the fatigue life and the load effect.

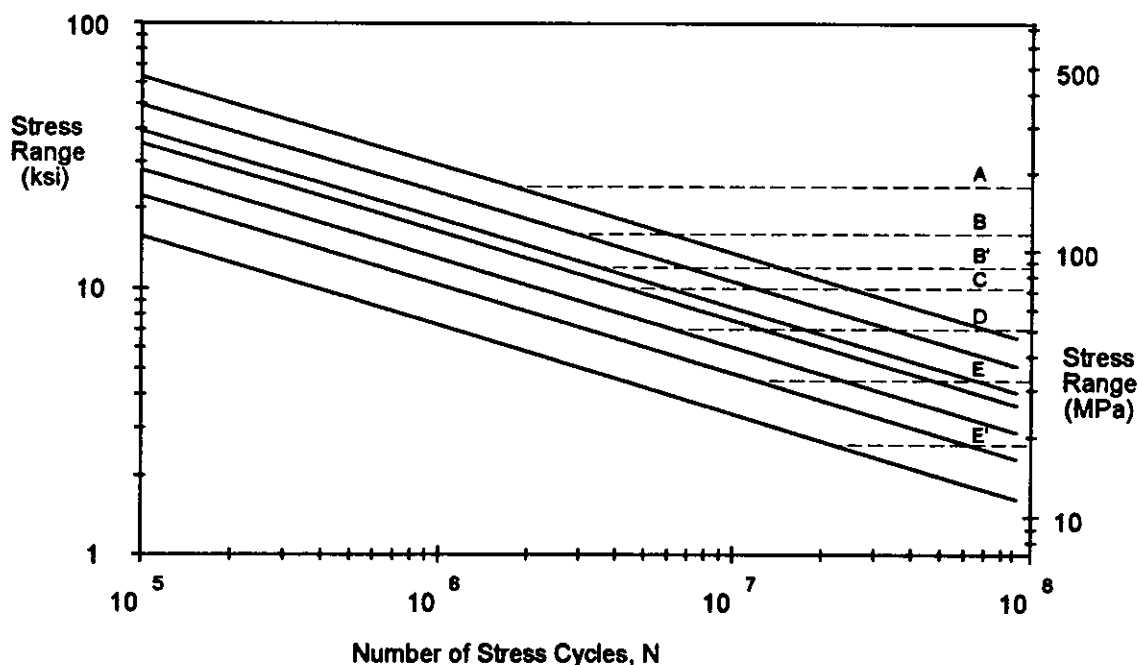


Figure 18 Fatigue rules according to the AASHTO Specification [28]

Figure 18 shows the fatigue life curves given by the AASHTO specification. Pictorials and an associated table are provided that enable the designer to assign a given detail to one of the fatigue categories shown in Fig. 18. The similarities between the ECCS and AASHTO approaches are obvious: both use a log stress range vs. log number of cycles representation; the slope constant of the curves is generally 3; pictorials are used in conjunction with the stress range vs. cycles information. The fatigue strength curves shown were selected on the basis of the mean of the test data less two standard deviations, the same procedure as used in the ECCS specification. Comparison of Figs. 16 and 18 shows the major differences: ECCS uses 14 categories of fatigue detail, whereas AASHTO uses eight; for large numbers of cycles,

the treatment is different in the two approaches. As has already been noted, the ECCS specification can use slope constants of either zero, 3, or 5 in this region. The AASHTO approach is to cut off the -3 slopes at various levels of fatigue life, and then simply use a zero slope. The ECCS specification also includes one category that has a slope different from all the others. It is presented separately from Fig. 16 and is not shown here.

The use of 14 fatigue classifications in the ECCS approach as compared to only eight by AASHTO should not be taken to imply a greater level of accuracy in the former. In the ECCS case, after establishing the top and bottom stress range categories, the decision was simply to provide intervals corresponding to the subdivision of one decade on the vertical scale by a factor of 20.

Leaving discussion of the other differences between the two specifications for the time being, a simple design example can be used to illustrate use of the fatigue strength information.

EXAMPLE 2

The overhead crane in a small manufacturing operation uses a simply-supported crane girder of 8 m span. The section used for the girder is to be made by fillet-welding three plates into an I-shape. Welding will be done automatically, with no stop-start positions within the beam length. The flange plates are 350 mm wide by 22 mm thick and the web plate is 306 mm by 14 mm. (The moment of inertia of this section is $448 \times 10^6 \text{ mm}^4$.) The main use of the crane will be to transport a 300 kN ladle from one end of the shop to the other. The crane travels in such a position that the crane girder receives a maximum 80% of the total load as a reactive force. It can be assumed that this force comes onto the girder as a single concentrated load. Information from the owner is that the crane will make no more than two trips per hour at this load level, this will be the only significant load, the work schedule will not exceed 10 hours per day five days per week, and the design life of the building is 40 years.

Is the fatigue life of this crane girder satisfactory? Use the ECCS specification.

Solution:

1. Number of stress cycles (equals number of load cycles, in this case) –

$$N = (2 \text{ cycles/hr.}) (10 \text{ hr./day}) (5 \text{ days/wk.}) (52 \text{ wk./yr.}) (40 \text{ yr.}) = 208\,000 \text{ cycles.}$$

2. Detail classification – According to the ECCS specification, this is Detail Category 125. From Fig. 16, read the Detail Category 125 line at $N = 200\ 000$ cycles to find that the permissible stress range is approximately 260 MPa.

3. Calculate actual stress range –

$$\sigma_{\min} = 0$$

$$\sigma_{\max} \quad M = PL/4 = (300 \times 10^3 \text{ N} \times 0.8) (8\ 000 \text{ mm})/4 = 480 \times 10^6 \text{ N mm}$$

$$\therefore \sigma_{\max} = M y/I = (480 \times 10^6 \text{ N mm}) (175 \text{ mm})/(448 \times 10^6 \text{ mm}^4) = 188 \text{ MPa}$$

$$\text{Thus, } \Delta\sigma_r = 188 - 0 = 188 \text{ MPa.}$$

Since the actual range of stress (188 MPa) is less than the permissible range of stress for this detail (260 MPa), the situation is satisfactory.

Comments:

1. The number of stress cycles is not always equal to the number of load cycles. Designers should be alert for cases where a single passage of load produces more than one stress cycle, as could occur, for example, when a multiple axle vehicle traverses a member or when continuous beams are used.
2. Since stress due to dead load is always present in the member, the change in stress ($\Delta\sigma_r$) is always simply equal to the change in stress produced by the moving (i.e., live) loads.
3. Another way of looking at the problem is to compare the number of cycles that would be permitted at the actual stress range of 188 MPa with the number of cycles that actually occur. In this example, the number of cycles permitted by the ECCS specification for a stress range $\Delta\sigma_r = 188$ MPa is $N = 588\ 000$ cycles, obtained from Fig. 16 or calculated as shown in Section 3.5.

3.5 Fracture Mechanics Analysis of Fatigue

In Section 2, *Basic Fracture Mechanics Analysis*, it was put forward that brittle fracture and fatigue are crack growth phenomenon that are characterized by the same parameter, K . As such, it should be possible to use the fracture mechanics method of analysis to deal with the fatigue strength problem.

The crack growth law was identified in Section 2 as

$$\frac{da}{dN} = A \Delta K^m \quad (6)$$

where a = crack length

N = number of cycles

A, m = numerical constants determined from regression analysis of test data.

ΔK = change in stress intensity factor corresponding to a given change in stress range. In Section 2, this was also written (Eq. 5) as

$$\Delta K = W Y \Delta \sigma \sqrt{\pi a} \quad (5)$$

Integration of Eq. 6 gave the following expression for crack growth propagation (see also Section 2):

$$N = \frac{1}{A} \int_{a_i}^{a_f} \frac{1}{\Delta K^m} da \quad (7)$$

where a_i and a_f are the initial and final crack length, respectively. Making the substitution for ΔK , this becomes:

$$\begin{aligned} N &= \frac{1}{A} \int_{a_i}^{a_f} \frac{1}{[W Y \Delta \sigma \sqrt{\pi} \sqrt{a}]^m} da \\ &= \frac{1}{A} \Delta \sigma^{-m} (\sqrt{\pi})^{-m} \int_{a_i}^{a_f} \frac{1}{(W Y \sqrt{a})^m} da \end{aligned}$$

The terms $1/A$ and $(\sqrt{\pi})^{-m}$ are constants. Since the final crack size is always very large as compared to the initial crack size, any term appearing with the limit a_f can be neglected since the limit will appear with a negative power. The terms W and Y vary with the crack length, and of course the term \sqrt{a} also contains the crack length. However, for a given geometry and starting crack size the term within the integral is also a constant. Designating the product of all of the constant terms as M and using the more common notation $\Delta \sigma_r$ instead of $\Delta \sigma$, the result can be written finally as

$$N = M \Delta \sigma_r^{-m} \quad (8)$$

or, alternatively, as

$$\log N = \log M - m \log \Delta \sigma_r \quad (9)$$

Equation 9 defines a sloping straight line on a plot of log stress range versus log number of cycles. This is precisely what is observed in the physical tests. See, for example, Figures 13, 14, and 15.

Equations 8 or 9 can be used to calculate explicit values of the number of cycles for a given stress range, or *vice versa*. This is particularly convenient when using the ECCS Specification, where the permissible stress range at 2×10^6 cycles is used to designate the detail category. Labeling this as DC (detail category) and using the value $m = 3$, the constant M in Eq. 8 can be written as $M = 2 \times 10^6 (\text{DC})^3$. Thus, if we want to obtain the permissible number of cycles for a given stress range, Eq. 8 becomes

$$N = (2 \times 10^6) (\text{DC})^3 \Delta\sigma_r^{-3}$$

or, more conveniently,

$$N = 2 \times 10^6 \left[\frac{\text{DC}}{\Delta\sigma_r} \right]^3 \quad (10)$$

Alternatively, if we wish to determine the permissible stress range for a given number of cycles, Eq. 8 can be written as

$$\Delta\sigma_r = \left[\frac{2 \times 10^6}{N} \right]^{1/3} (\text{DC}) \quad (11)$$

Application of Eq. 10 and 11 can be made in Example 2. In step 2 of the Solution, the permissible stress range for $N = 208\,000$ cycles for this Detail Category 125 is calculated according to Eq. 11 as

$$[(2 \times 10^6) / (208\,000)]^{1/3} \times 125 \text{ MPa} = 266 \text{ MPa.}$$

In Comment 3 of Example 2, the number of cycles permitted for $\Delta\sigma_r = 188 \text{ MPa}$ is calculated as

$$2 \times 10^6 (125/188)^3 = 588\,000 \text{ cycles..}$$

The AASHTO specification likewise provides a means of calculating the permissible stress range for a given number of cycles, or *vice versa*. In that specification, the constant M in Eq. 8 is provided for each fatigue category; it is given in Table 1. The values shown in that table, where the constant is called A , are to be applied when calculations are in U.S. Customary units, of course. If necessary, the conversion between MPa and ksi stress units

(6.89) can be made at the appropriate location. Also shown in the table is the value of the stress range that identifies the horizontal portion of each curve, the so-called threshold stress.

Table 1 Constants for use with Figure 18

Detail Category	Constant, A	Threshold Stress (ksi)
A	2.5×10^{10}	24.0
B	1.2×10^{10}	16.0
B'	6.1×10^9	12.0
C	4.4×10^9	10.0
C'	4.4×10^9	12.0
D	2.2×10^9	7.0
E	1.1×10^9	4.5
E'	3.9×10^8	2.6

EXAMPLE 3

The beam whose failure surface is illustrated in Fig. 11 was one of a series of nine tested [31]. Using the test data, the regression line expressing the relationship between fatigue life and stress range was determined to be $\log N = 10.03 - 2.73 \log \Delta\sigma_r$. The flaws from which the cracks initiated were generally circular and the measured average size (U.S. Customary units) was 0.053 in. Use fracture mechanics analysis to verify the experimentally obtained regression line.

Solution:

It has been noted that the final size of the crack will not be influential in the result of Eq. 7. This means that the stress intensity modifiers W and Y in Eq. 5 can be taken as a constant. Calling the product $WY = C$, and substituting for ΔK in Eq. 7 gives

$$N = \frac{1}{A} C^{-m} \Delta\sigma_r^{-m} \int_{a_i}^{a_f} a^{-m/2} da$$

$$= \frac{1}{A} C^{-m} \Delta\sigma_r^{-m} \left. \frac{a^{1-m/2}}{1-m/2} \right|_{a_i}^{a_f}$$

Calling $m/2 - 1 = q$, this can be written as

$$N = \frac{1}{A} C^{-m} \Delta\sigma_r^{-m} \frac{1}{q} (a_i^{-q} - a_f^{-q})$$

Since the final crack size is always very large as compared with the initial crack size, the term a_f can be neglected because it appears with a negative power in this equation. Thus, the crack propagation equation can be further simplified to

$$N = \frac{1}{A} C^{-m} \Delta\sigma_r^{-m} \frac{1}{q} a_i^{-q}$$

Rolfe and Barsom [8] suggest that the constant of proportionality, A , in the crack growth equation (Eq. 6) can be taken as 3.6×10^{-10} for ferrite-pearlite steels. They also suggest the value of C in the stress intensity factor expression can be taken as $2.0/\sqrt{\pi}$ for a circular crack in a plate of infinite width, and that the term m can be taken as 3, i.e., $q = (m/2) - 1 = 0.5$. The combined multipliers of $\Delta\sigma$ are the term M in Eq. 8, and we can now solve for this value. Using the alternative form, Eq. 9, we solve for $\log M$ as –

$$\begin{aligned} \log M &= \log \left[\frac{1}{A} C^{-m} \frac{1}{q} a_i^{-q} \right] \\ &= \log \left[\frac{1}{3.6 \times 10^{-10}} \left(\frac{2}{\sqrt{\pi}} \right)^{-3} \frac{1}{0.5} (0.053)^{-0.5} \right] = 10.23 \end{aligned}$$

Thus, the equation of the fatigue strength line as obtained using the experimental data and a fracture mechanics analysis is

$$\log N = 10.23 - 3 \log \Delta\sigma_r$$

This is in good agreement with the fatigue strength line obtained from the experimental data exclusively ($\log N = 10.03 - 2.73 \log \Delta\sigma_r$).

Comments:

Obviously, this type of exercise is not directly useful to a designer since it requires knowledge of the type and size of flaw that is likely to result in fatigue crack growth and failure.

However, the results of this analysis and others like it do identify that the behaviour observed in the laboratory can be substantiated by an analytical prediction—the fracture mechanics analysis. It gives confidence in the prediction of cases not tested experimentally when those predictions are based on presumption of reasonable starting flaw sizes and shapes.

4. FATIGUE ASSESSMENT PROCEDURES FOR VARIABLE STRESS RANGES

In all of the discussion so far, it has been implicit that the stress range at the detail under investigation can be established easily and that counting or predicting the number of cycles is straightforward. As might be anticipated, things are not simple in either of these categories: loading histories are usually quite complex. The designer has to deal with the reality that stress ranges of different magnitude take place at the detail and that these stress ranges are applied for varying numbers of cycles. A way of dealing with these problems is outlined in this Chapter.

4.1 Cumulative Fatigue Damage

In this section, a method is presented that accounts for the damage that results when different stress ranges are applied for various lengths of time. Although both linear and non-linear damage theories are available, the one that is customarily used in civil engineering practice is a linear theory that is easy to understand and apply and which gives satisfactory results. This is the linear damage rule first proposed by Palmgren in 1924 and further developed by Miner in 1945 [32]. It is known as the Palmgren-Miner rule, and it simply assumes that the damage fraction that results from any particular stress range level is a linear function of the number of cycles that takes place at the stress range. The total damage from all stress range levels that are applied to the detail is, of course, the sum of all such occurrences. This can be written in equation form as:

$$\sum \frac{n_i}{N_i} = 1 \quad (12)$$

where n_i = number of cycles that take place at stress range level i

N_i = number of cycles that would cause failure at stress range level i .

The rule is obviously very simple. It has two major shortcomings [32]; it does not consider sequence effects and it is independent of the amplitude of the stress cycles. To at least some degree, both of these factors are not consistent with observed behaviour. However, when residual stresses are high and when plasticity is restricted (usually the case in structural

engineering applications), it is known that these factors have only a small influence. Moreover, the approach gives reasonable correlation with test data and it has the considerable advantage that it is easy to use. Both of the specifications used as references in this primer [15, 28] advise that the Palmgren-Miner rule can be used to account for cumulative damage. It should also be noted that the term "failure" in these definitions is not intended to be taken literally. It is to be interpreted as the permissible fatigue life, that is, the value represented by the mean life less two standard deviations on the log stress range vs. log number of cycles plot.

EXAMPLE 4

The beam of Example 2 was designed, fabricated, and erected when the owner decided that, in addition to the loads that had already been stipulated, it will be necessary for the crane be able to accommodate one trip per hour at a load level of 350 kN. (See Example 2 for all other details). Is the fatigue life of this crane girder still satisfactory?

Solution:

1. Number of cycles at the old load level was 208 000 ($= n_1$)
2. Number of cycles to failure at the old load level was 588 000 ($= N_1$)
3. Number of cycles at the new load level is –
 $N = (1 \text{ cycle/hr.}) (10 \text{ hr./day}) (5 \text{ days/week}) (52 \text{ weeks/yr.}) (40 \text{ yr.})$
 $= 104 \text{ 000 cycles } (= n_2).$
4. Number of cycles to failure at the new load level –

By proportion, the stress range for the 350 kN load is $(350/300) (188 \text{ MPa}) = 219 \text{ MPa}$. Using Fig. 16 for Detail Category 125, or by calculation $(2 \times 10^6)(125/219)^3 = 372 \text{ 000}$, the number of cycles that would be permissible at the stress range of 219 MPa is $N_2 = 372 \text{ 000}$.

5. Finally checking Eq. 12

$$\sum \frac{n_i}{N_i} = 1 \text{ or,}$$

$$\frac{n_1}{N_1} + \frac{n_2}{N_2} = \frac{208 \text{ 000}}{588 \text{ 000}} + \frac{104 \text{ 000}}{372 \text{ 000}} = 0.35 + 0.28 = 0.63$$

Since the total effect ("damage") of the two different stress ranges is less than 1.0, the crane girder is still satisfactory.

Sometimes it is convenient to express the Miner-Palmgren cumulative fatigue damage rule (Eq. 12) in terms of an equivalent stress range. We wish to calculate an equivalent stress

range, $\Delta\sigma_e$, that acts for the number of cycles to which the detail is actually subjected, N , and has the same effect as the variable stress ranges. We recognize that it is a requirement that $N = \sum n_i$. Using the stress range versus number of cycles relationship expressed by Eq. 8, for the particular case of the equivalent stress range, $\Delta\sigma_e$, the relationship can be written as –

$$N = M \Delta\sigma_e^{-m}$$

For a general stress range case, $\Delta\sigma_i$, the relationship is

$$N_i = M \Delta\sigma_i^{-m}$$

If we call $\gamma_i = n_i / N$, that is, γ_i is the fraction that any particular portion of the stress range is of the total number of cycles, then the Miner summation (Eq. 12) can be expressed as –

$$\sum \frac{\gamma_i N}{N_i} = 1.0$$

Making the substitutions for N and N_i in terms of stress, we have –

$$\sum \frac{\gamma_i M \Delta\sigma_e^{-m}}{M \Delta\sigma_i^{-m}} = 1.0 \quad \text{or,}$$

$$\Delta\sigma_e^m = \sum \gamma_i \Delta\sigma_i^m \quad \text{and}$$

$$\Delta\sigma_e = \left[\sum \gamma_i \Delta\sigma_i^m \right]^{1/m} \quad (13)$$

Reference 15 (ECCS specification) expresses this result as –

$$\Delta\sigma_e = \sum_{i=1}^k \left[\frac{\Delta\sigma_i^m n_i}{N} \right]^{1/m} \quad (14)$$

and in Reference 28 (AASHTO specification), the equivalent stress range is written as

$$S_{re} = S_{r\text{Miner}} = \left[\sum \gamma_i S_{ri}^3 \right]^{1/m} \quad (15)$$

It should be clear by inspection that Equations 14 and 15 are identical to Eq. 13.

EXAMPLE 5

Use the equivalent stress method to determine the percentage of life that has been expended by the loading applied to the beam of Example 4.

Solution:

All of the necessary data are available in the solutions to Examples 2 and 4. In summary, these are –

$$n_1 = 208\,000 \text{ cycles}$$

$$n_2 = 104\,000 \text{ cycles}$$

$$\Delta\sigma_1 = 188 \text{ MPa}$$

$$\Delta\sigma_2 = 219 \text{ MPa}$$

$$N = 208\,000 + 104\,000 = 312\,000 \text{ cycles}$$

Selecting the expression given by Eq. 14 to calculate the equivalent stress range –

$$\Delta\sigma_e = \left[\frac{(188^3 \times 208\,000) + (219^3 \times 104\,000)}{312\,000} \right]^{1/3}$$

$$= 199.4 \text{ MPa, say, } 200 \text{ MPa.}$$

For this Category 125 Detail and the equivalent stress range of 200 MPa, the number of cycles to failure can be calculated (Eq. 10) as –

$$2 \times 10^6 \left[\frac{125}{200} \right]^3 = 488\,280 \text{ cycles}$$

Since the actual number of cycles is 312 000, the percentage of life expended is $(312\,000/488\,288) 100\% = 63.9\%$.

Comments:

The same result was also seen in the solution to Example 4, where the Miner's summation was 0.63. Whether the solution proceeds by the method shown in Example 4 (Miner's summation) or by that shown in Example 5 (equivalent stress range method) is simply a matter of choice.

4.2 Analysis of Stress Histories

Situations often arise where the applied loads create stress levels and stress counts (number of cycles at a given stress level) that are much more complicated than those given in Example 4. For example, if the crane in Example 4 is carried by a continuous beam over several intermediate supports, more than one stress cycle is applied per trip at a given location. This results because loading adjacent spans causes stress cycles in addition to the cycle created when the crane passes directly over the location under examination. For this more general case, one trip is termed a loading event and the stress variation at a given point in the structure during such an event is called a stress history.

Very complicated stress histories can be caused by loading events such as the passage of a train over a bridge or a wave hitting an offshore oil platform. Furthermore, the occurrence of a loading event brings about different stresses within different elements in a structure, and, in addition, the number of cycles per loading event may be related to the type and location of the element under consideration. Also, local conditions, such as bolted connections loosened by vibration, may magnify the effects of dynamic loading. Thus, many different stress histories may need to be evaluated for a complete fatigue assessment of a complex structure.

In fields other than civil engineering, elaborate stress measurements are often taken on actual structures subjected to service loading in order to overcome uncertainties associated with calculated values of stresses in elements. Unfortunately, it is rare that such measurements are carried out on civil engineering structures, usually because of the cost. Consequently, civil engineers generally resort to stress analysis using load models and dynamic magnification factors provided in codes and standards.

The curve shown in Fig. 19 (a) is an example of stress variation in an element subjected to a loading event. Typically, simple analyses result in stress histories having fewer peaks than shown in this figure, whereas stress measurements usually reveal more complex stress histories.

The information shown in Fig. 19 (a) cannot be used directly in the Palmgren-Miner rule, Eq. 12, without application of a stress counting method in order to tabulate values for the number of cycles, n_i , for different stress range levels. This tabulation is called a stress spectrum. Several counting methods have been developed for various applications, and Reference 23 provides a summary of these methods. The most widely used is the so-called rainflow counting method [33], named for its analogy of rain drops flowing down a pagoda roof. Peaks and troughs for one loading event are numbered in Fig. 19 (b) and this history is rotated 90 degrees in Fig. 19 (c) in order to perform the rainflow analysis.

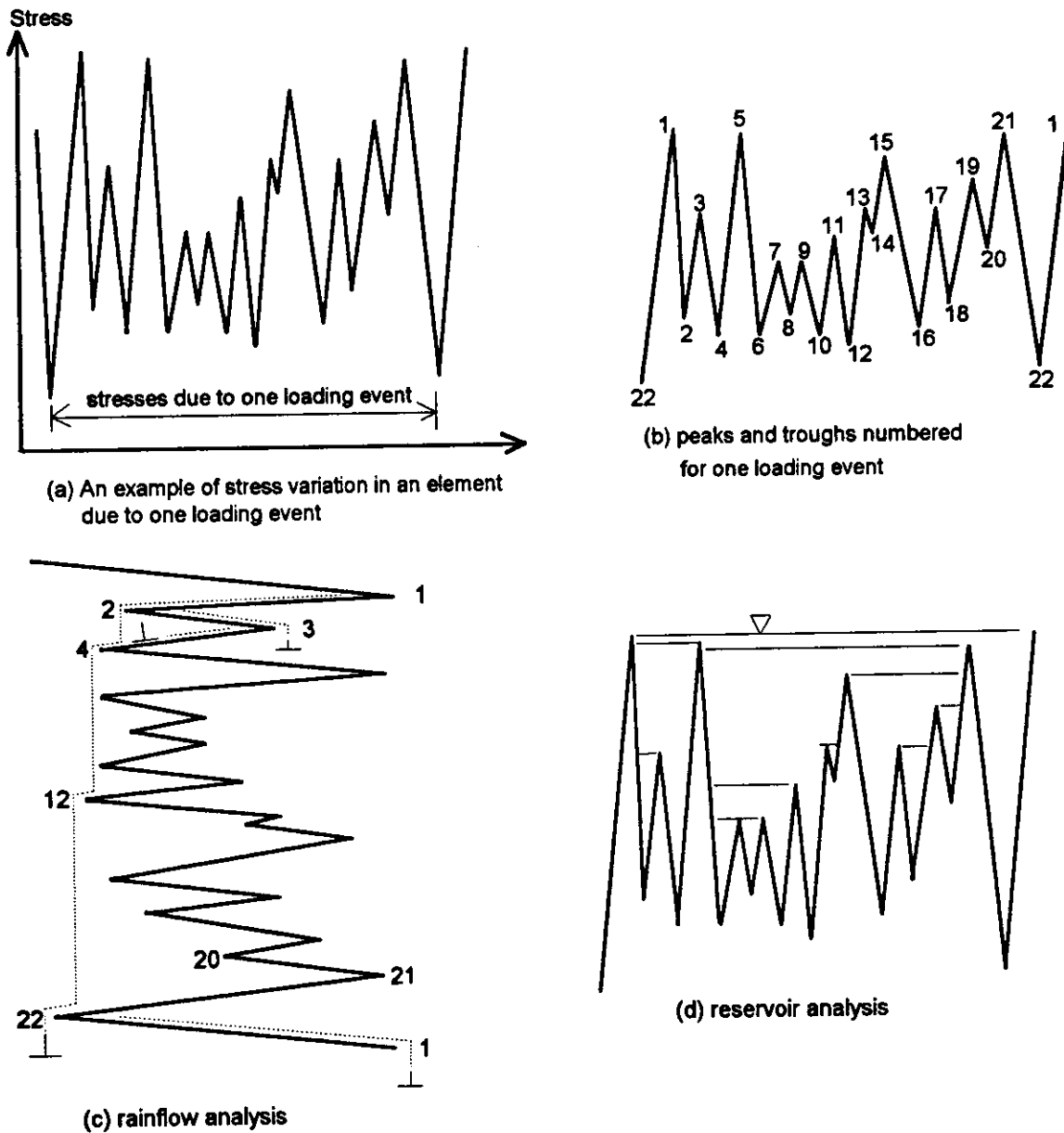


Figure 19 Analysis of stress histories

The following rules apply to rainflow counting:

1. A drop flows left from the upper side of a peak or right from the upper side of a trough and onto subsequent "roofs" unless the surface receiving the drop is formed by a peak that is more positive for left flow or a trough that is more negative for right flow. For example, a drop flows left from point 1 off points 2, 4 and 12 until it stops at the end of the loading event at point 22 since no peak is encountered that is more positive than

- point 1. On the other hand, a drop flows right from point 2 off point 3 and stops since it encounters a surface formed by a trough (point 4) that is more negative than point 2.
2. The path of a drop cannot cross the path of a drop that has fallen from above. For example, a drop flowing left from point 3 stops at the horizontal position of point 2 because a path coming from point 2 is encountered.
 3. The horizontal movement of a raindrop, measured in units of stress from its originating peak to its stop position is counted as one half of a cycle in the stress spectrum.

An alternative method, called the reservoir method because of its analogy of water contained in reservoirs formed by peaks draining successively out of troughs, is shown in Fig. 19 (d). To start, imagine that the area bounded by the highest peak in the loading event forms a reservoir of water contained by it and the same peak in a following, identical, loading event. Using the numbering shown in part (b) of Fig. 19, this is point 1. Next, drain water from the reservoir out of the lowest trough in the spectrum, point 22 in Fig. 19 (b). Water caught between other peaks forms smaller reservoirs. Drain water successively out of the lowest troughs in the loading event until all reservoirs have been drained. The vertical distance, measured in stress units, between a high water level and the drain (trough) that lowers it is counted as one full cycle in the stress spectrum.

The rainflow and reservoir methods give identical results provided that rainflow counting begins with the highest peak in the loading event, as is shown in Fig. 19. Generally, rainflow counting is more suited to computer analyses of long stress histories, whereas the reservoir method is most convenient for graphical analyses of short histories.

EXAMPLE 6

The values of the peaks for the stress history shown in Fig. 19 are given below. Apply (a) rainflow counting and (b) reservoir counting in order to identify the stress ranges in the stress spectrum. Finally, (c) evaluate the effects of one million loading events of this stress history acting on a beam that uses a manually welded longitudinal fillet weld to connect the flanges to the web (ECCS category 100 detail).

The given data are --

Solution: (b) Reservoir counting method

Drain from Trough No.	Water Level at Peak	Stress Range (MPa)
22	1	93
12	21	77
4	5	75
16	15	66
2	3	37
18	17	37
10	11	36
6	7	27
20	19	26
8	9	19
14	13	9

Note that these stress ranges are the same as were determined in part a) using the rainflow counting method.

Solution: (c) Cumulative damage using the Palmgren-Miner rule

Stress Range $\Delta\sigma$ (MPa)	Fatigue Resistance $N = (100/\Delta\sigma)^3 \cdot 2 \times 10^6$ cycles	Damage Due to 1×10^6 Loading Events, n_i/N
93	2 490 000	0.402
77	4 381 000	0.228
75	4 741 000	0.211
66	6 957 000	0.144
37 (twice)	39 480 000	0.051
36	42 870 000	0.023
27	101 600 000	0.010
25	113 800 000	0.009
19	292 600 000	0.003
9	2.7×10^9	0.000

Damage summation: $\sum n_i/N = 1.08 \geq 1.0$

Comments:

This analysis indicates that the fatigue evaluation has failed, meaning that the element may not withstand one million loading events. At this point, the designer has several remedial possibilities. In order of importance these are:

1. A better design detail should be investigated. Often, fatigue problems can be traced to poor initial design detail choices. In this example, the use of automatic welding, which means no

intermediate stop-start positions, would increase the fatigue strength of this element by 25% since the fatigue category changes from ECCS 100 to ECCS 125. If this change could be made, in this example the damage summation would be 0.55, a substantial reduction, and the detail would then pass the fatigue evaluation.

2. Measures which reduce stresses due to dynamic loading should be studied. Such measures could involve employing continuous construction, avoiding short members near application of loads, reducing the number of expansion joints, improving road surfaces on road bridges and improving three-dimensional load-carrying capacity. Such measures may require sophisticated stress analysis methods in order to evaluate and incorporate their effects in the fatigue evaluation.
3. A more detailed fatigue analysis could be carried out. This is covered next, in Section 4.3.
4. Only as a nearly last resort, the thickness of the member could be increased in order to lower the stresses. Note that if this is done, the fatigue strength may also decrease, see Section 6.3.

4.3 Fatigue Limits

Two limits are described in this Section, the constant-amplitude fatigue limit and the cut-off limit. The constant-amplitude fatigue limit (CAFL) is the more important of the two because it determines the relevant case for variable-amplitude stress spectra; see Fig. 20. Case 1 refers to the situation where all cycles are above the CAFL. Case 2 covers stress spectra which contain stress ranges that are both above and below the CAFL. In Case 3, all stress ranges are below the CAFL.

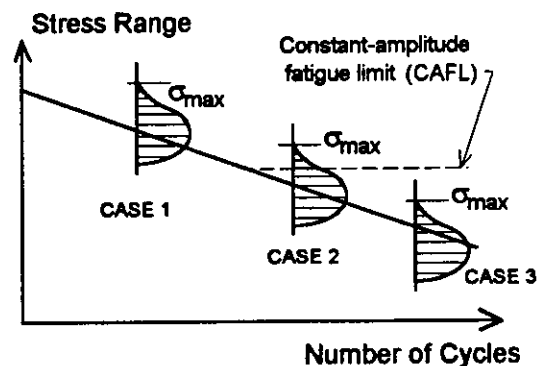


Figure 20 Three cases of variable amplitude stress spectra

Methods for analysis of spectra in Case 1 are the same as the discussion and examples given thus far. Options for Case 2 spectra are described below. Spectra which fall into Case 3 do not require a fatigue assessment provided that no stress range due to any other loading event exceeds the CAFL. If a stress range in a spectra which resulted from another loading event does exceed the CAFL, then Case 3 spectra should be considered in the same way as Case 2 spectra.

Case 2 spectra are most often associated with situations where long fatigue lives are required. For example, structures such as bridges, offshore platforms, chimneys, and overhead highway signs are often subjected to millions of loading events. It is difficult to guarantee that values of all stress ranges will remain less than the value for the CAFL throughout the service life of the structure.

Two options are possible for the analysis of Case 2 spectra. Firstly, it can be assumed, conservatively, that all cycles contribute to crack propagation in the element from the first cycle of fatigue loading. This is equivalent to assuming that the value for the fatigue threshold stress intensity factor is zero. For this option, analysis proceeds in a fashion identical to the analysis required for Case 1. The analysis in Example 5 adopted this option. In effect, this option assumes that the fatigue strength curve continues below the CAFL with a slope constant of 3.

The second option for analysis of Case 2 spectra is based on a more logical assumption that not all cycles in the spectrum will contribute immediately to crack propagation. This assumption is equivalent to admitting the presence of a non-zero value for the fatigue threshold stress intensity factor. As crack propagation proceeds, more and more cycles in the spectrum will exceed the threshold stress intensity factor range until all cycles in the spectrum contribute to crack propagation at a certain crack length.

International opinion as to how the analysis should proceed in the Case 2 second option is not unanimous. This is due to a lack of test data at sufficiently long fatigue lives so as to be able to verify proposed analyses. Furthermore, fracture mechanics analyses are hindered by difficulties in estimating values for the threshold stress intensity factor under conditions of high tensile residual stress that vary with crack length. The ECCS Recommendations allow the use of a slope constant, m , of 5 for stress ranges below the CAFL (see Fig. 16). However, recent work indicates that this may be unsafe for stress spectra applied to large beams with welded longitudinal attachments [34]. Nevertheless, test data for all other cases investigated indicate that use of the slope constant of 5 is acceptable. It remains to be seen whether the best rule is the first option or the second option qualified by a provision for exceptional cases. More research and testing is needed.

The second limit discussed in this Section, the cut-off limit, is used to discard small stress cycles from the stress spectrum. Small cycles in the spectrum do not contribute significantly to fatigue damage: it is considered that by the time cracks grow to a length where

these stresses would induce stress intensity factor ranges greater than the threshold stress intensity factor range, the vast majority of fatigue life has been expended.

The importance of the cut-off limit is greatest when automatic stress measuring equipment is used. This equipment is capable of measuring several thousand small cycles per loading event. When the number of small stress cycles (having values less than half of the CAFL) is greater than two orders of magnitude more than the number of large cycles, the Palmgren-Miner damage summation may result in an overly conservative evaluation. The ECCS Recommendations suggest a cut-off limit at the stress level which corresponds to the intersection of the fatigue strength curve ($m = 5$) with one hundred million cycles.

EXAMPLE 7

Consider again the stress spectrum given in Example 6. What would the ECCS detail category have to be in order that the assessment fall into a Case 3 situation?

Solution:

In the ECCS Recommendations, the constant amplitude fatigue limit (CAFL) starts at 5×10^6 cycles. Since the method of identifying the fatigue category in this specification is to cite the fatigue strength at 2×10^6 cycles, and since the slope constant of the fatigue life line is to be taken as 3, the detail category can be calculated by asking what the maximum stress range in the problem (93 MPa, see Example 6) would be at 2×10^6 cycles. Thus, using Eq. 11, the detail category (DC) is identified as:

$$DC = 93 \times \left(\frac{5 \times 10^6}{2 \times 10^6} \right)^{1/3} = 126$$

Although detail category 125 provides slightly less strength than required, for most designers this would still be an acceptable choice.

Choose ECCS category 125 (Note point 1 in comments to solution for Example 6, Part (c)).

EXAMPLE 8

Recalculate the damage summation for Example 6 using a cut-off limit of 40 MPa for ECCS category 100.

Solution:

In the solution of Example 6, it was implicit that all stress cycles are damaging. This is conservative, as has been discussed, and the ECCS Recommendations allow that all stress

ranges less than the cut-off limit (see Fig. 16) can be disregarded. First, verify that cut-off limit is 40 MPa. Since two slopes are now involved (3 and 5), first establish the CAFL, that is, the stress range at 5×10^6 cycles. Using Eq. 11;

$$\text{CAFL} = [(2 \times 10^6) / (5 \times 10^6)]^{1/3} \times 100 \text{ MPa} = 73.7 \text{ MPa}$$

Now, following the same procedure but using the slope of 5;

$$\begin{aligned} \text{Cut-off limit} &= [(5 \times 10^6) / 1 \times 10^8]^{1/5} \times \text{CAFL} \\ &= [(5 \times 10^6) / 1 \times 10^8]^{1/5} \times 73.7 = 40.5 \text{ MPa} \cong 40 \text{ MPa (as expected)} \end{aligned}$$

Recalculate damage summation --

Stress Range $\Delta\sigma$ (MPa)	Fatigue Resistance $N = (100/\Delta\sigma)^3 2 \times 10^6$ cycles	Damage due to 1×10^6 Loading Events n_i/N
93	2 490 000	0.402
77	4 381 000	0.228
75	4 741 000	0.211
66	6 957 000	0.144

$$\text{Damage summation: } \sum n_i/N = 0.985 \leq 1.0 \quad \text{Satisfactory}$$

The fatigue assessment now indicates that the element can withstand one million loading events.

EXAMPLE 9

Recalculate the damage summation for Example 6 taking into account the cut-off limit and a slope constant, m , of 5 below the CAFL.

Solution:

The CAFL is 74 MPa for a detail category of 100. Therefore the fatigue resistance in terms of number of cycles, N , needs to be recalculated for all stress ranges between 74 MPa and 40 MPa. The complete table is as follows:

Stress Range $\Delta\sigma$ (MPa)	Fatigue Resistance cycles	Damage due to 1×10^6 Loading Events n_i / N
93	2 490 000	0.402
77	4 381 000	0.228
75	4 741 000	0.211
66	8 860 000	0.113

Damage summation: $0.954 < 1.0$ Satisfactory

Comments:

1. The fatigue resistance for the stress ranges greater than 74 MPa is calculated using $(100/\Delta\sigma)^3 2 \times 10^6$ cycles, as in Example 6. In this example, the only fatigue resistance that needs to be recalculated is that for the 66 MPa stress range. In a development similar to that used for Eq. (10), this is calculated as $(CAFL / \Delta\sigma)^5 5 \times 10^6$.
2. Since the element was already found to be satisfactory using the cutoff limit of 40 MPa and a constant slope of 3 (Example 8), the examination herein is unnecessary. However, this will not always be the case.

5. INSPECTION AND REPAIR OF FATIGUE CRACKS

This section provides recommendations directed toward helping the engineer decide what to do if a crack is discovered in a steel structure. Decisions should be based upon a scientific understanding of crack propagation, combined with knowledge gained through practical experience of examining steel structures and dealing with cracks found in those structures. Earlier chapters have provided the scientific foundation; this chapter discusses more practical considerations. Generally, if a crack is found in a steel structure, more careful inspection will reveal additional cracks in similar elements. If no action is taken to eliminate the cause of cracking, more cracks usually appear at other locations. For these reasons, the discovery of a crack should be taken seriously by the inspection team and reported immediately to the engineer responsible for the structure. Quick fixes, carried out by untrained personnel, often worsen the problem.

5.1 Identifying the Causes of Cracking

Before any action is taken, an attempt should be made to determine the causes of cracking. Although this course of action seems obvious, often it is not followed in practice. Fatigue crack-growth mechanisms are activated by factors such as large numbers of stress ranges, severe stress concentrations, dynamic magnification (impact), corrosion damage, inappropriate fabrication procedures, bad welding processes, and large defects. Almost always, more than one factor contributes to a critical situation.

The parameters that effect the stress ranges at a given location can be difficult to quantify. For example, the effect of truck passages over a worn expansion joint at the end of a bridge may be impossible to evaluate without strain-gauge measurements. Stress ranges brought about by temperature changes and other types of deformation-induced stresses (sometimes called secondary stresses) present similar problems. Occasionally, signs of high stresses, such as wear marks on contact surfaces or visible out-of-plane movement, indicate that the structure is subjected to high stress ranges. Often, the most accurate evaluation possible can do no more than provide a list of candidate factors ordered according to their importance. In some instances, examination of a crack segment removed from the structure can assist a specialist in the determination of the most probable causes (see reference [35]).

The extent to which stress ranges are known usually determines the accuracy of estimates of the number of fatigue cycles applied to the structure. If possible, this information should be checked against recommendations for fatigue strength in the design specification in order to determine whether cracking would be expected under such circumstances. Note that if cracking is visible, it may be assumed that there is no remaining fatigue life, and therefore a check can be performed using standard relationships between stress range and total fatigue life. The reason for making such a check is that if fatigue cracking cannot be explained in this way, all sources of fatigue loading may not have been identified. The fact that the structure has survived without fatigue failure for a given period may be the only piece of information available that is completely certain.

When fatigue loading information and code recommendations cannot explain fatigue cracking, other factors not covered by fatigue strength curves—such as large defects due to poor fabrication methods and the effects of corrosion—may have influenced cracking. Special requirements exist for the fabrication of steel structures subjected to fatigue loading. For example, eccentricities due to fit-up that may be acceptable for some structures might seriously weaken a structure subjected to fatigue loading. The structure should be examined for evidence of large eccentricities, corrosion damage, and fabrication-induced discontinuities.

Note that lack of weld penetration which is oriented transversely to the direction of fatigue loading is equivalent to an initial crack. (See Figure 6.)

5.2 Taking Appropriate Measures

Repairing a cracked element is an obvious option, but others should also be considered. Appropriate measures could also include implementation of damage tolerance strategies and element replacement. When damage tolerance strategies are used, no immediate action is taken to repair the crack or replace the element. Repair can be delayed, thereby making it possible to avoid repairs at inconvenient times. Furthermore, this strategy often provides the opportunity to determine the causes of cracking more precisely. However, damage tolerance should not be employed when rupture of the element would cause general collapse of the structure; when continued cracking would endanger human life through increased deformations (for example, an increased risk of derailment due to cracking of a railway girder); when monitoring crack growth at regular intervals is not possible; or when further cracking may substantially increase repair costs.

In order to ensure that a damage tolerance strategy is successful, additional measures are recommended. Fracture mechanics analyses should be employed to predict crack growth and to determine critical crack lengths, i.e. crack lengths at which fracture would be expected. Laboratory testing of specimens (Charpy V-notch, CT, etc.) made from steel taken from the structure may be needed. Crack measurement equipment should be calibrated and verified on a regular basis. Also, any modifications to the structure or changes to the applied loading should be assessed in order to verify that the structure can safely tolerate further cracking.

Repair of cracks, when carried out correctly, may result in an adequate solution to fatigue cracking provided that the steel quality is appropriate for both present and future service conditions. However, when repairing fatigue cracks, it is important to keep in mind that repair welding is rarely successful, and therefore weld repair should be employed as a last resort when no other solution is possible. The following is a list of measures which have been employed successfully for steel structures containing fatigue cracks. These measures are ordered (roughly) from best to worst.

- Place cover plates over the crack in order to provide a load path for forces and to restrict movement of the crack surfaces during fatigue loading. These cover plates should be placed on both sides of the cracked plate and they must be attached with pretensioned structural bolts.

- Drill a hole at the end of the crack and fill the hole with a structural quality bolt and pretension the bolt according to code provisions for bolted assemblies. See reference [35] for guidance regarding appropriate hole diameters. Care must be taken to ensure that the crack front is intercepted by the hole.
- Cut out and refabricate parts of elements in order to reproduce the same conditions that existed at the crack site before cracking occurred. Employ fatigue-strength improvement methods to increase fatigue resistance. This measure is most effective for cases in which fatigue cracks have grown from weld toes and when cracking in another, unimproved location is unlikely.
- Air-arc gouge the crack, fill the gouged area with weld metal, grind away weld reinforcement, polish smooth and inspect for weld defects using ultrasonic and X-ray inspection technology. This measure should be accompanied by some modification which reduces fatigue stresses in the region surrounding the crack.

Finally, any measure which lowers the stress ranges in the area around the crack will contribute to the success of a repair. Care should be taken to ensure that cracking at other locations is not triggered as a result of these measures. Such consequences are most likely when the local stiffness of the structure is modified, thereby altering the sensitivity of the structure to dynamic loading.

When damage tolerance strategies are not appropriate and when no repair option can be implemented, replacement of the cracked element may be warranted in those situations where it is possible to remove and replace the element. In the presence of corrosive environments, and when there is any doubt regarding the grade of steel used in the structure, employ a steel grade that is more suited to the situation.

Replacement using a larger element than that originally present will result in lower stresses at the location where the crack was detected, and, for this reason, use of a larger element is often warranted. However, a larger element alters the stiffness of the structure. Consequently, the effects of this change in stiffness should be studied in order to ensure that problems are not created elsewhere.

After removal of the cracked element, all connections should be inspected for cracking. Reuse old connection material only if it can be demonstrated that it has not been damaged by the incidence of cracking in the element. Although connections may not be cracked, they may be damaged due to excessive movement. Do not reuse bolts that were used in the old element for connecting the new element.

Fabrication work on the new element should be performed where adequate quality of workmanship can be assured. Work on site should be avoided, especially if such activity does not contribute to reducing built-in-stresses and eccentricities. Therefore, site work should be limited to actions such as drilling under-sized holes to fit and other joining techniques that are intended to ensure good fit and satisfactory alignment.

5.3 Avoiding Future Cracking Problems

If fatigue cracking has been discovered at one location in a structure, it is likely to be present at other similar locations. Consequently, if nothing is done to improve conditions at those places, development of fatigue cracks is probable in the future. Therefore, such locations should be identified and measures for improvement of their fatigue resistance should be considered.

Measures that lower the stress ranges in the structure are the most effective way of preventing further crack growth. Care should be taken to ensure that susceptibility to fatigue cracking is not increased elsewhere as a result of these measures. Such consequences are most probable when the local stiffness of the structure is modified, thereby altering the response of the structure to vibration and other loading.

Effective measures for avoiding future cracking problems usually fall into one of the following categories:

- reduction of applied stress ranges
- reduction of dynamic magnification (impact)
- reduction of number of cycles of damaging stress ranges
- decrease in vibration through damping, addition of mass or a change in restraint
- use of fatigue-strength improvement methods at critical locations.

Corrosion-induced cracking can be avoided by protecting the structure from the environment, not allowing water and debris to become trapped on the structure, by providing adequate drainage (for example, for de-icing salts) and, finally, through modifying areas sensitive to electrolytic action.

The following general precautions are recommended for the structure as a whole:

- Identify areas in the structure where cracking would create a dangerous condition. Use the same criteria as those used to judge whether further cracking can be tolerated for

implementation of a damage tolerance strategy. Mark these areas for modification and inspection.

- If new information is received regarding the structure or if structural modifications are significant, reconsider decisions made regarding the management of the structure.
- Inspect repair locations regularly in order to verify the effectiveness of repair measures.
- Create conditions whereby the structure can be inspected as easily as possible. This involves measures such as keeping the structure clean, providing safe access to critical locations, and designing modifications considering in-service inspection.
- All modifications should be designed with the goal of making the structure as fail-safe as possible. Fail-safe means that the structure can tolerate failure of one or more elements before a catastrophic condition arises. This condition must be preceded by a period which is long enough to identify cracking and to take appropriate action.

6. SPECIAL TOPICS

6.1 Role of Residual Stress

Steel structures that are fabricated by welding contain "residual" or "locked-in" stresses that have been introduced as a result of the welding process. These have considerable influence on the propagation of fatigue cracks. The main effect is to significantly reduce the effects of the applied stress levels, *per se*, for standard weldable structural steels. For modern codes, this has brought about a return to the simple stress range vs. cycle life model for fatigue strength suggested by Wöhler over one hundred years ago. Furthermore, independence of steel grade justifies the use of the relatively large data base of laboratory results taken from tests of different steel grades produced in different countries. During recent modifications to fatigue codes, code developers have taken advantage of such opportunities and, consequently, fatigue design guidelines have been greatly simplified and harmonized internationally.

Consider a weld laid down as shown in Fig. 21. As the weld cools, it tries to contract. However, since the plate and the weld must maintain compatibility of length, the plate restrains the weld during the cooling and contraction process. This puts the weld, and a relatively small volume of plate adjacent to the weld, into tension. Meanwhile, the main portion of the plate is being pulled down by the contracting weld, thereby placing it into compression. These stresses are called "residual" stresses. Since there are no external forces

applied during this process, the equilibrium condition of the cross-section must be reflected in the balance of residual tensile stress and the volume over which it acts and that for the residual compressive stress and its associated volume. The actual distribution and magnitude of the residual stress pattern depends upon many factors, including the strength of the steel and the weld metal, the geometry of the connected parts, the size of the weld relative to the connected parts, and so on. The important fact, however, is that the magnitude of the tensile residual stress can reach the yield strength of the material.

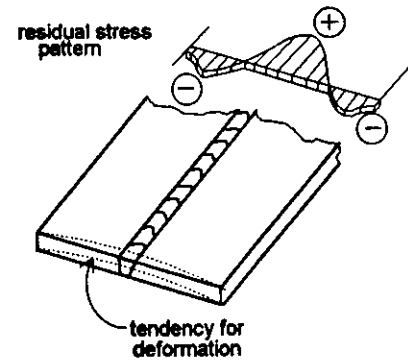


Figure 21 Residual stresses in a welded plate

Regions of residual tensile stress exist, for example, at the junction of the flange and web of a beam that has been built up by welding the component parts together. Since this junction is also the most likely location of the flaws that are likely to be the source of fatigue crack growth, this means that the flaw is under a condition of initial stress even before load is applied. For the usual condition wherein this initial stress is at the yield stress level, this means that stress range, rather than the maximum applied stress, the stress ratio (ratio of maximum stress to minimum stress), or some other parameter of applied stress, is the governing condition describing fatigue crack growth. This will be illustrated by the following numerical example.

EXAMPLE 10

Figure 22 shows a rectangular plate and its assumed residual stress pattern. (This could be an idealization of the flange of a welded beam). According to the designer, the plate will be subjected to a maximum tensile stress of 215 MPa and a minimum compressive stress of 122 MPa. Calculate the actual range of stress that will exist for a flaw at the center of the plate (junction of the web and flange of the welded beam). Compare this range of stress with the stress range that will be computed by the designer, that is, $+215 - (-122) = 337$ MPa.

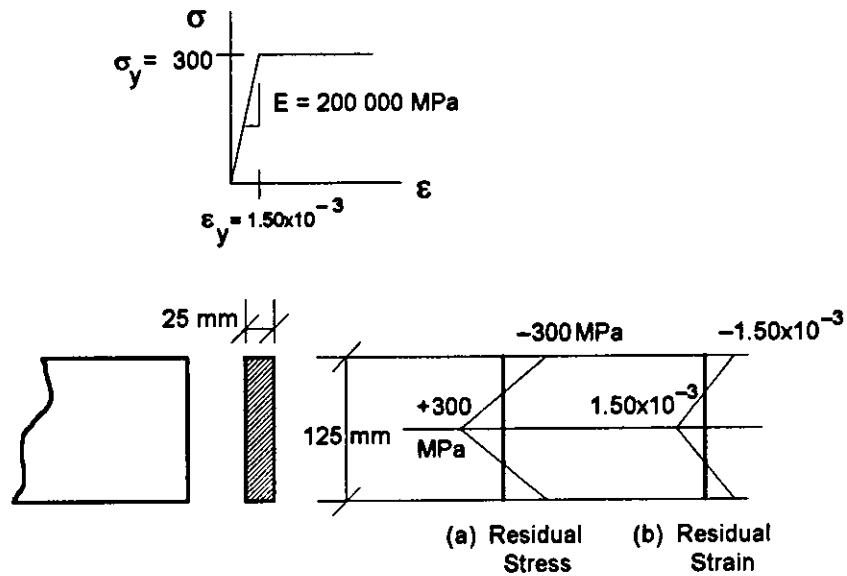


Figure 22 Initial stress condition in a welded plate

Solution:

1. Initial conditions—The initial pattern of residual stress is shown in Fig. 22 (a). It shows that the values of the initial stress are as high as the yield stress. Since the yield stress is not exceeded, however, the corresponding strains can be calculated from the elastic relationship, $\sigma = E \epsilon$, and these strains are shown in Fig. 22 (b). There is no force on the member, and we note (by inspection) that the condition $P = \int \sigma dA = 0$ is met.
2. Apply tensile force such that the design stress level is +215 MPa, i.e.,

$$P = \sigma A = 215 \text{ N/mm}^2 \times (25 \times 125) \text{ mm}^2 = 672 \times 10^3 \text{ N} = 672 \text{ kN}$$

During application of this force, which is the equivalent of the imposition of a uniform compressive strain over the residual strain of Fig. 22 (b), not all parts of the cross-section respond in the same way. Specifically, the relationship $\epsilon = \sigma / E$ will not be valid for those regions of the resultant strain diagram where the strain is greater than the yield strain. Figure 23 shows the residual strain, Fig. 23 (a) is Fig. 22 (b) repeated, the strain imposed by the tensile force, Fig. 23 (b), the resultant strain, Fig. 23 (c), and the corresponding stress diagram, Fig. 23 (d).

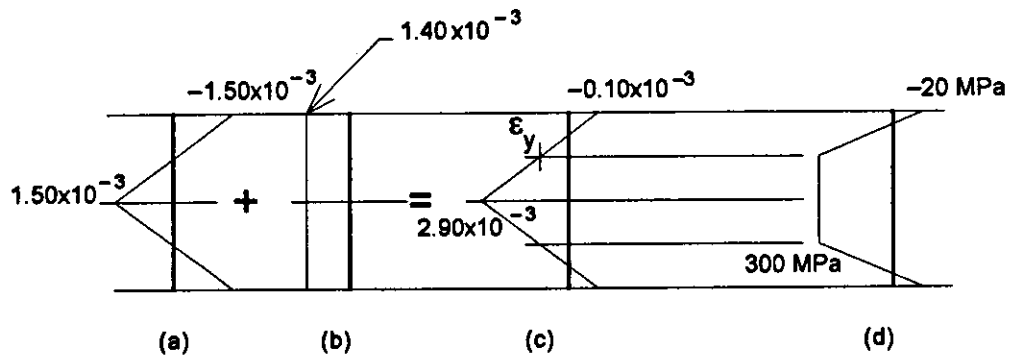


Figure 23 Superimposed strain (step 2) and corresponding stress

The value of the uniform strain corresponding to imposition of the applied force, 1.40×10^{-3} , was determined by trial so to satisfy the requirement that $\int \sigma dA = 672\,000\text{ N}$. That the integral is satisfied can be confirmed by first calculating the dimensions of the stress diagram, Fig. 23 (d), and then calculating the force volume obtained when the stress diagram is superimposed on the cross-section.

3. Now, apply a force such that the nominal stress in the cross-section goes to 122 MPa compression. This requires that the 672 kN force be removed and an additional force of $(-122\text{ N/mm}^2) \times (25 \times 125)\text{ mm}^2 = -381 \times 10^3\text{ N}$ be applied. Thus, the change in force is $\Delta P = (672 + 381) = 1053\text{ kN}$. As before, a uniform strain must be applied of sufficient magnitude such that $\int \sigma dA = P = 381\text{ kN}$. By trial, this has been determined to be a strain of 1.70×10^{-3} .

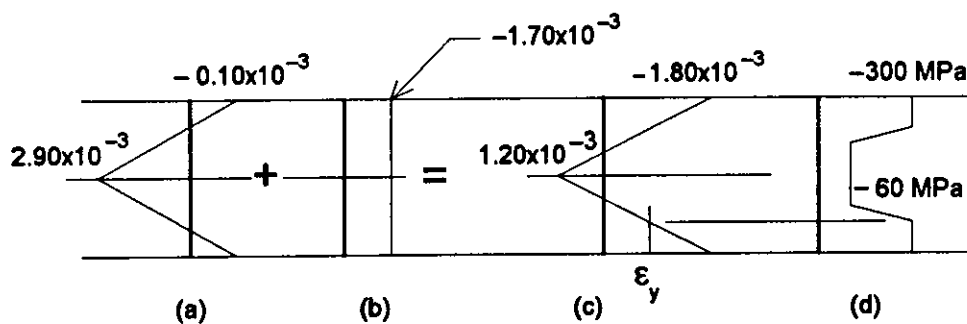


Figure 24 Superimposed strain (step 3) and corresponding stress

Figure 24 (a) shows the strains that existed at the end of step 2. Figure 24 (b) is the uniform compressive strain that must be applied to satisfy the requirement that a force of 381 kN be imposed. The resultant strains are shown in Fig. 24 (c). The reader should verify the stress values shown in Fig. 24 (d) and that the imposition of these stresses on the cross-section does in fact produce the value 381 kN.

4. Finally, examine the stresses in the mid-depth fibre of the cross-section. As shown in Figure 25, the stress initially was 300 MPa, that is, it was the yield value. Upon initial loading to 672 kN force, the stress remained at this value, even though the strains increased as shown in Figure 25. The unloading that occurred in Step 3 took the stresses down to 40 MPa compression. Thus, the actual change in stress at the mid-depth fibre was from

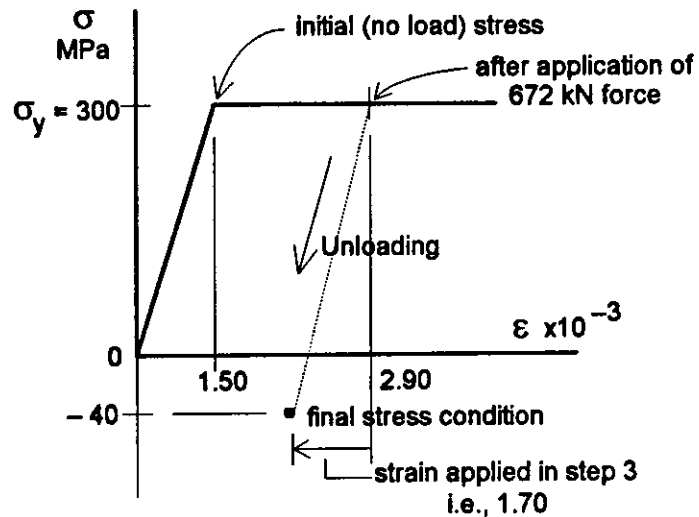


Figure 25 Strains and stresses at mid-depth fibre

+300 MPa down to -40 MPa, a total change of 340 MPa. The result is that the actual change of stress, 340 MPa is equal (nearly) to the change of stress calculated by the designer, 337 MPa. (The difference between the two values is attributed to round-off errors in the calculations.)

To summarize, in large welded structures there are very high tensile residual stresses near fatigue crack sites and their presence significantly reduces the effects of applied stress levels and steel grade upon crack propagation for standard weldable structural steels. As a result, it is generally agreed that stress range is the only dominant stress parameter. However, there has been a great deal of discussion regarding the best way to treat the following cases:

- The influence of compressive applied stresses
- The fatigue strength of non-welded elements
- The fatigue strength of stress-relieved welded elements
- The difference between results taken from testing small specimens and those taken from testing full-scale elements.

Most of the differences between various codes can be traced to different interpretations of the effect of residual stresses (and other built-in stresses) upon the fatigue strength of structural elements. A selection of approaches to these cases is described next.

Nearly all fatigue guidelines for steel structures recommend that non-welded elements, stress-relieved welded elements, and welded elements be treated in the same manner when the applied stress ranges are tensile. When the applied stress ranges are compressive, or partly compressive, recommendations vary. According to the AASHTO recommendations [28], it is possible to ignore all fully compressive stress ranges. However, if a part of the stress range is tensile, then the whole stress range must be considered. European recommendations suggest that the whole stress range should be employed, regardless of whether it is completely or partially compressive, when welded elements are assessed. The new Eurocode 3 (EC 3) [37] allows a reduction of the compressive stress range to 60% of its magnitude for non-welded and stress relieved elements. The ECCS recommendations [15] are the most conservative; they recommend that 100% of the stress range be used for all elements and all cases. Table 2 summarizes the different provisions.

Table 2 Percentage of applied stress range to be used in different fatigue codes

Code	Elements	Fully Tensile	Tension and Compression		Fully Compressive
AASHTO	All	100	100	100	0
EC3	As-Welded	100	100	100	100
	Non-Welded or Stress-Relieved	100	100	60	60
ECCS	All	100	100	100	100

Authors of the AASHTO provisions argue that, even if fatigue cracks start within tensile residual stress fields, under fully compressive loading cracks will eventually stop when they propagate beyond the influence of these stresses. The developers of the EC 3 document note that a crack growing from an as-welded joint in an element may be dangerous when applied stress ranges are full compressive. Indeed, some test elements have failed due to cracks growing under fully compressive applied loading. Also, the EC 3 provisions reflect an attempt to accommodate those cases where there are no high tensile residual stresses.

For the ECCS document, it was decided to provide conservative recommendations because in most complex structures the magnitudes of built-in stresses are unknown. Built-in stresses do not only originate from welding related residual stresses, but they may also be caused by other effects such as lack of fit, settlement of supports, temperature gradients, and inefficient expansion joints. Therefore, it was decided that no advantage should be given to

cases where applied stresses are in compression or where elements contain no tensile residual stresses.

The final point in this section relates to the physical testing of fatigue specimens. Compared with elements that have no tensile residual stresses, the presence of tensile residual stress near potential crack sites in an element reduces its fatigue strength, especially at long lives. Small test specimens may not contain the same high level of tensile residual stress found in full-scale elements. For this reason, some research programmes have concentrated upon testing of full-scale elements in order to establish code recommendations. Therefore, results taken from tests of small specimens should be employed with caution for design assessments. Also, when test programs are employed to obtain a more accurate fatigue strength relationship than is provided in fatigue codes, when it is possible the test specimen should have the same dimensions as the element under consideration for the real structure.

6.2 Combined Stresses

Throughout the discussion so far, it has been emphasized that the stresses to be used in the fatigue life evaluation are those corresponding to the nominal stress as obtained from a strength of materials level of analysis. The detail classification stipulated by the governing specification includes the effect of local stress concentrations due to weld shape, discontinuities, triaxial conditions, and so on. Only in exceptional cases, around large openings, for example, will a more sophisticated analysis be required. Occasionally, also, it might be necessary to investigate the combined effect of normal and shear stresses.

For a case in which both normal and shearing stresses are present in significant quantities at a given location, the principal stresses should be calculated and that stress range then used in the fatigue life evaluation. (Normal stress is defined as the stress perpendicular to the direction of the potential fatigue crack.) Of course, for this examination to be necessary, both the normal and shear stresses must be concurrently present at that location during a given loading event.

In unusual situations, shear stress alone can be significant. The test results show that, although the general relationship between stress range and number of cycles still exists, the slope of the relationship for shear loading is significantly different than for normal stresses. The slope is now 5, rather than 3. Otherwise, the design or evaluation proceeds as before. This approach is included in all of the specifications referred to in this document.

When normal and shear stresses are present at the same location but do not occur simultaneously under a given loading event, the individual components of damage can be added according to a Miner's summation, as follows:

$$\left[\frac{\Delta\sigma_e}{\Delta\sigma_r} \right]^3 + \left[\frac{\Delta\tau_e}{\Delta\tau_r} \right]^5 \leq 1 \quad (16)$$

where σ and τ refer to normal stresses and shear stresses, respectively. The subscript e means a calculated equivalent stress range (see Eq.13, for example) and the subscript r refers to the permissible stress range for the detail.

6.3 Effect of Size on Fatigue Life

Most of the test results upon which the fatigue life rules are based were done on specimens where the component parts were in the order of 12 to 25 mm thick. Fabricated steel structures often use plate thickness considerably greater than this, however, particularly in the case of flanges of welded built-up beams. It is generally agreed [19,20,22] that the fatigue resistance of thicker elements is less than that of thinner elements. Although a thicker element will have a greater statistical chance of containing flaws, this does not seem to be the main reason for the decrease. Rather, it has to do with differences in the residual stress patterns that will result when using thicker plates and from the observation that the stress concentration at the weld toe increases as plate thickness increases [39].

At the present time, the only recognition of the decrease fatigue life with plate thickness is made by stipulating a lower fatigue detail category when plate thickness exceeds 25 mm. The AASHTO Specification, for example, reduces the fatigue category from E to E' in certain cases when the plate thickness exceeds 25 mm [28]. The category for base metal at the end of partial length cover plates is reduced from E to E' when the thickness exceeds 20 mm. Finally, it should also be noted that the effect of plate thickness upon fatigue life has only been observed for transverse joints—for longitudinal joints the effect may be opposite to that just indicated.

6.4 Environmental Effects

The effects of the environment upon the fatigue life of steel members may show up in one of several ways. Corrosion can produce local effects that cause stress concentrations. For instance, corrosive products (e.g., brine) can drip down from an upper level to a lower level and produce both a local reduction in cross-section and a notch effect. Old railway bridge

members sometimes show this type of corrosion. For example, the top surface of the lower flange of a girder can often show local changes in cross-section as brine has dripped down from the upper levels. (Ice and salt were formerly used as a refrigerant in railway rolling stock). It is not uncommon to see depressions in the order of 25 to 50 mm diameter, with depths in the order of 3 to 8 mm. In extreme cases, particularly with members that were not very thick to begin with (e.g., bracing members, lacing bars), the local corrosion may completely penetrate the member. Although these are not desirable situations, they are similar to the introduction of a hole; as such, they do not introduce a particularly severe flaw into the member. Since this type of corrosion effect will generally be an issue in the case of evaluation of old bridges, a value judgment can be made as to how much to degrade the fatigue life as compared with an uncorroded member. Fisher et al. have reported on the fatigue life of a number of corrosion-notched beams [38]. The ratio of corroded part to original thickness ranged from 0.2 to 0.8. Although the number of test data in which the corrosion effect has been specifically examined is quite limited, Fisher et al. recommend that all corrosion-notched details be carefully examined for the possibility of fatigue cracking. They suggest that if the corrosion reduces the thickness by more than one-half, fatigue cracking is likely to start at the notch rather than at the location of net section produced by the rivet or bolt holes.

There are also instances in which the entire cross-section has been corroded, more or less in a uniform way. The source of the corrosion in these cases is a more general source, such as high humidity, usually in a salt-laden atmosphere, or corrosive fumes in proximity to chemical process plants. In the case of a general reduction in cross-section, the designer can evaluate the fatigue life based on an estimate of the reduced cross-section. Of course, the designer should be alert to the presence of notches in this case also.

A very significant effect of corrosion can be the direct effect of the corrosive element upon on fatigue crack growth. At stress levels greater than the endurance limit, this effect is to set up corrosive reactions within the crack, thereby accelerating the growth. The other mechanism is the growth of existing surface pits in the presence of a corrosive environment, thereby increasing the severity of the stress concentration. Both of these mechanisms have the effect of reducing the fatigue life of an element or detail below that which it would have been in air. Corrosion may also have the effect that the constant-amplitude fatigue limit may no longer be present.

The effect of a corrosive environment upon crack growth or as it increases stress concentrations has not received much attention, particularly in civil engineering applications. The available laboratory test results, often done at relatively high test rates, do not indicate

any significant effect [35]. Moreover, experience in the field does not support the need for inclusion of special rules for bridges or similar structures that are operating in the types of corrosive environments normally associated with that type of structure. In two specific cases, the consequences of operating in a corrosive environment are included explicitly in the design rules. Both of these are clear-cut—offshore structures and the drillpipe used in oil exploration. In both instances, the environment is severe—salt water—and its consequences cannot be avoided. There is not much test data available here either, however, and it must be recognized that corrosion and its effect on fatigue life is time-dependent. Thus, testing in this area takes even longer that it does for the normal situation of testing in air. Designers of civil engineering structures in particularly harsh environments should take special care that detailing of the structure minimizes the possibility of locations for fatigue and that maintenance will be properly thought out.

Many civil engineering structures must operate in low temperature environments. Again, there are very few test data in this area. The work of Fisher et al. [38] did include some tests in which a portion of the fatigue crack growth was done under very low temperatures (-40°C and -73°C). The study showed that the low temperature did not result in sudden fracture until the cracks had become very large.

In summary, it can be concluded that the civil engineering structures most likely to have to endure corrosive environments, especially bridges, can be designed in accordance with the rules that have been developed on the basis of tests in air. Evaluation of existing structures in which corrosion has affected the cross-section can be done by applying judgement and using the results of those tests that are available [38]. In the case of new structures, great care should be taken to ensure that corrosion products from roadway decks are directed away from the members and that spray from traffic either above or below the bridge is cleaned up periodically. Detailing should be done with a view to minimizing those locations where corrosion products can form and sit, especially in crevices.

6.5 Fatigue Cracking from Out-of-Plane Effects

Most of the discussion in this primer has centered around the influence of normal stresses on pre-existing flaws or cracks in a fabricated steel element. The assumption has been that the stresses can be calculated, usually at an elementary level. In many instances, however, fatigue crack growth results from the imposition of deformations, not stresses. Although it is possible in some of these cases to calculate a stress range, this is usually after the fact, i.e., after a fatigue crack has already been detected. The designer is not likely to be able to identify

the need for such a calculation in the course of his work. As will be seen, this type of fatigue crack growth results from the imposition of relatively small deformations, usually out-of-plane, in local regions of a member. These deformations are not anticipated in the design process. The main defense against this source of cracking is proper detailing, and this, in turn, is dependent on experience.

Figure 26 illustrates the phenomenon with an example. Standard practice for many years was to cut transverse stiffeners short of the bottom (tension) flange so as to not introduce a relatively severe detail for fatigue if the stiffener is welded to the flange at that location. (There are also practical reasons for cutting the stiffener short: the stiffener will have to be made to a precise length if it is to extend from flange to flange.) The height of the

gap is usually quite small. If lateral movement of the top flange relative to the bottom flange should take place, large strains can be imposed in the gap region because of the significant change in stiffness between the stiffened and unstiffened (gap) regions of the web. The strains that typically are produced are so large [40] that it may take relatively few cycles for a crack to propagate. The flange movement could be the consequence of transverse forces in a skew bridge, but more often it is a consequence of shipping and handling.

The detail to Fig. 26 shows the crack emanating from the weld toe at the bottom of the stiffener. Often, the crack will also extend across the toe of the fillet weld at the underside of the stiffener and for some distance into the web. Up to this stage, the crack is more or less parallel to the direction of the main stress field that the girder will see in service. Thus, if the source of the displacement-induced fatigue can be identified and eliminated, then further growth of the crack is unlikely. However, if crack growth has gone on for some time, the crack may have turned upwards or downwards in the web, and thus be aligned in the most unfavorable orientation with respect to service load stresses.

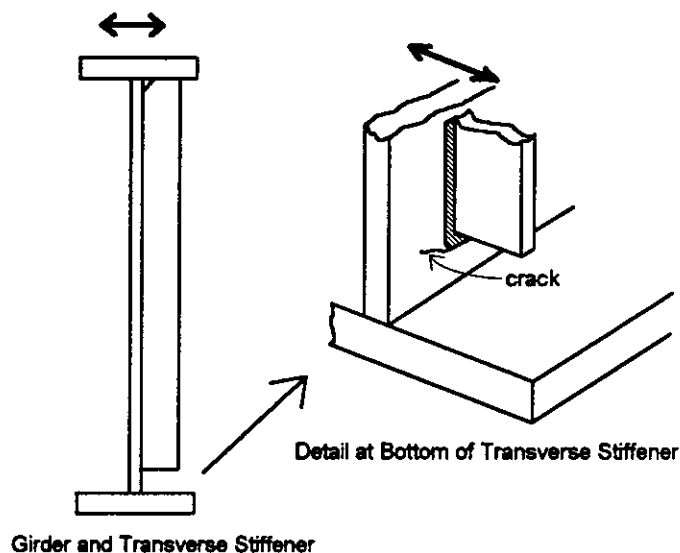


Figure 26 Example of fatigue cracking due to out-of-plane movement

The detail just described (Fig. 26) has been the source of many fatigue crack locations in the past. New designs can handle the situation in different ways, reducing the possibility of fatigue crack growth due to this cause.

An effective way of dealing with the type of crack shown in Fig. 26 is to drill holes at the end of the crack, thereby changing the sharp crack front to a "crack" front with an extremely large radius. See Fig. 27. In preparation for drilling, the area should be cleaned and a dye penetrant used to locate the extremity of the crack as accurately as possible. The hole should then be drilled with its trailing edge at the location identified as the crack front. In this way, it can be reasonably certain that the hole has indeed intercepted the crack front. A typical hole size used for this procedure is 12 mm. The hole should be drilled carefully and then, if necessary, lightly ground to remove scratches and burrs. If the hole is simply left open, the location can be easily monitored for the possibility of further crack growth. Alternatively, a high-strength bolt can be placed in the hole and pretensioned. The introduction of high compressive stresses into this region is an effective way of increasing the fatigue life at this locality. A disadvantage is that if the original fatigue crack continues to grow, it cannot be observed until it appears from under the bolt head or washer.

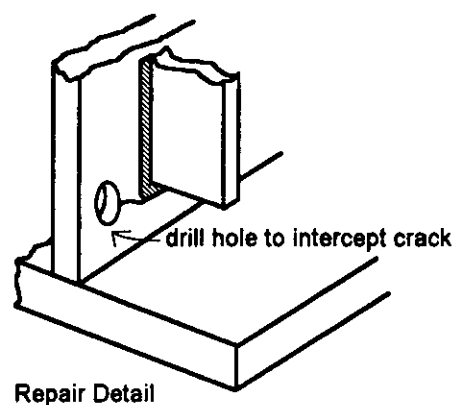


Figure 27 Repair of a fatigue crack

Another illustration of a case in which out-of-plane movement can produce fatigue cracks is shown in Fig. 28, where a floor beam is attached to a connection plate that is welded to the web of a girder. Under the passage of traffic, the floor beam will rotate as shown. As this rotation occurs, the bottom flange of the floor beam will tend to lengthen and the top flange will tend to shorten. Lengthening of the bottom flange will not be restrained because it is pushing into the web of the girder, which is flexible in this out-of-plane direction. However, because the top flange

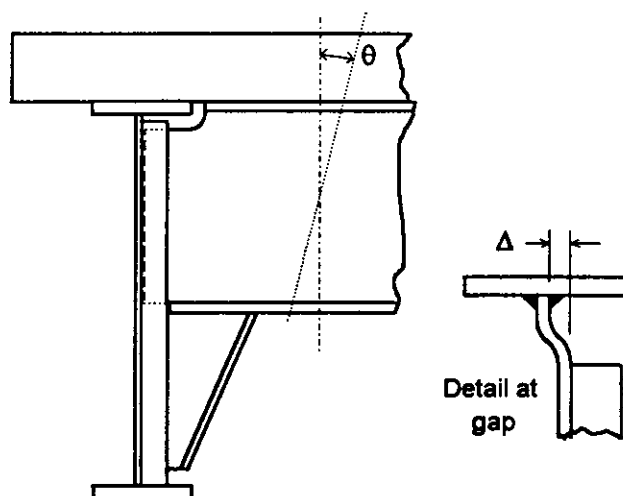


Figure 28 Floor beam to girder connection

of the girder is restrained by the deck slab, shortening of the top flange of the floor beam can only be accommodated by deformation within the gap at the top of the connection plate. This type of deformation is shown in the detail in Fig. 28.

The situation hypothesized in Fig. 28 has been confirmed by field measurements taken by Fisher [40]. Moreover, the field study showed that each passage of an axle caused a significant stress range at the top of the connection plate. In this situation, fatigue cracks could develop either at the weld at the top of the connection plate or at the web-to-flange fillet weld of the girder, or both. The residual tensile stress in this small gap would tend to be very high because of the proximity of the two welds. It can be expected that fatigue cracks could occur under relatively few cycles of load, although of course the fatigue life will depend largely upon the deformation, Δ , that actually takes place as a result of the rotation of the floorbeam.

EXAMPLE 11

Given:

Figure 28 illustrated a floor beam to girder connection where out-of-plane cracking could occur. The detail is repeated here, as Fig. 29. The web – flange fillet weld is a Category 71 detail according to the ECCS specification. The web plate thickness is $t = 12$ mm, the length of the gap is $L = 15$ mm, and a measurement of the displacement of the gap shows that $\Delta = 0.003$ mm. What is the fatigue life of this detail?

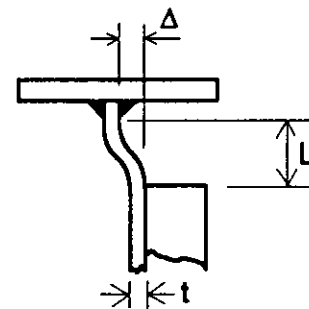


Figure 29 Example 11

Solution:

Application of moment-area principles, or reference to a design handbook, will show that the moment at the end of a fixed ended beam which is displaced an amount Δ is

$$M = \frac{6 EI \Delta}{L^2}$$

$$\text{Thus, the stress is } \sigma = \frac{M y}{I} = \left(\frac{6 EI \Delta}{L^2} \right) \left(\frac{t}{2} \right) \left(\frac{1}{I} \right) = \frac{3 E \Delta t}{L^2}$$

Since the displacement Δ is varying, this can be interpreted as the stress range, $\Delta \sigma$. For the specific quantities given:

$$\Delta\sigma = \frac{(3)(200\,000\text{ MPa})(12\text{ mm})(0.003\text{ mm})}{(15\text{ mm})^2} = 96\text{ MPa}$$

The number of cycles for a detail category 71 that can sustain a stress range of 96 MPa can be calculated conveniently using Equation 11:

$$N = 2 \times 10^6 \left[\frac{DC}{\Delta\sigma_R} \right]^3 = 2 \times 10^6 \left[\frac{71\text{ MPa}}{96\text{ MPa}} \right]^3 = 809 \times 10^3\text{ cycles}$$

Comment:

This example shows that even a very small amount of out-of-plane displacement can have a significant effect on fatigue life. In this case, the fatigue life of this Category 71 detail is reduced by over one-half for the displacement of 0.003 mm.

There are many other sources of out-of-plane fatigue cracking or locations for secondary (uncalculated) stress. For example —

- **Restraint At Simple End Connections.** Many end connections are designed as "simple, that is, it is assumed that no moment is transmitted. However, even simple connections do carry some moment, and this means that the connection elements will deform under the moment. End rotation at web framing angles causes the angles to deform and load the rivets, bolts, or welds in ways not contemplated by the design. If the loading is cyclic, fatigue cracks may develop in the angles themselves or in the bolts, rivets, or welds. In the cases of the mechanical fasteners, prying forces develop that may cause fatigue cracking under the heads.
- **Floor Beam or Stringer Connections to Girders.**
- **Coped Beams.** In order to facilitate the easy connection of one flexural member to another, the flange of one of the members is often cut back, as is illustrated in Figure 30. (In other cases, the flanges may simply be narrowed: this is called a "blocked" beam.) In the case of coped beams, either the top or bottom flange, or both, may be coped. The cope is usually made by flame-cutting the material, and experience shows that this is often done in a less-than-satisfactory manner. The radius of the cope will often be small, and the cutting done unevenly. In addition to the

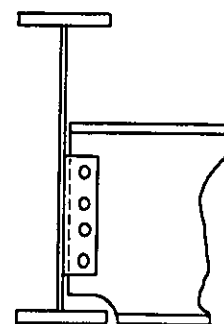


Figure 30 Bottom flange of floorbeam coped at connection to girder

potential for fatigue cracking created by such workmanship, the flame-cutting process can leave a region of hardened and brittle material adjacent to the cut.

The coped end of the beam is at a location of theoretical zero stress since the connection must necessarily be one that does not transmit moment and the shear force is carried by the web. Nevertheless, the region of the cope will have stresses due to bending because of the restraint at the connection. There are many examples of fatigue cracking at cope locations [26], and the best solution in the case of new designs is to avoid copes entirely. If copes must be included, the workmanship and inspection must be of a high standard. Specific information on the fatigue life of a coped beam can be found in Reference 41.

- **Rotation of Beam or Girder Flanges by Direct Loading.** The most obvious example of this is the case of railway beams or girders. Particularly in older members, it was common to place the ties directly on the top flange of the flexural members in the floor system. Thus, a stringer flange, for example, can be rotated as traffic passes over the structure. If the flange is too flexible in this direction, cracking can occur at the web-to-flange junction.

6.6 Quantitative Design Using Fracture Mechanics

The fatigue strength curves described in Chapter 3 are not capable of providing an engineer with information necessary for several special cases related to fatigue assessments. For example, these curves cannot evaluate the influence of an unusually large defect; they are not able to evaluate the influence of inspection precision upon fatigue reliability; they provide little help in fixing inspection intervals; and finally, they cannot be used to predict the remaining life of a cracked structure. Fracture mechanics provides the central analytical model employed in fatigue assessments for dealing with these aspects.

Some defects that may be rejected during standard fabrication controls would not, in reality, influence the performance of the structure. The economic consequences of remedial measures are often severe and resulting project delays can be long. Quality assurance provisions in many codes are based more upon accepted standard practice, experience, and detection capability than upon scientific accuracy.

Fracture mechanics offers a more rational means of defect assessment. In such analyses, the value for the initial crack length in Equation 7, Section 2.3 is normally taken to be equivalent to the size of the defect. Equation 7 is then integrated, usually numerically using equal increments of cycles, in order to determine cycle life. If the cycle life is greater than the number of cycles expected over the life of the structure, the defect may be regarded as being

acceptable. Reference 36 provides guidelines for appropriate values of W and Y for use in Equation 3 and for additional criteria, such as those which determine whether two closely spaced defects should be considered to be equivalent to one large initial crack.

A similar approach can be used for the design of structures when fabrication quality cannot be guaranteed and when it is known that inspection technology is unable to detect defects that are more severe than those normally known to occur in steel structures. In these evaluations, it is assumed that defects are present and the minimum detectable defect size becomes the initial crack size for use in Eq. 7. When the cycle life resulting from the integration is less than the number of cycles applied over the life of the structure, either the design is modified or inspection technology that enables greater precision is justified. Such analysis has been used to determine inspection criteria for steel structures in the North Sea, for example.

Often, determination of intervals between in-service inspections does not consider the behaviour of the structure if it were to contain a crack. Crack-growth curves can be predicted for all critical details in a structure, as shown schematically in Figure 31. Between the crack length when first detection is possible, a_0 , and the critical crack size, a_{cr} , a set number of inspections, n , should be performed. A constant crack-length increment, Δa , should be fixed rather than a constant time interval. The number of inspections should be determined using reliability analyses that take into account crack-detection probabilities and the consequences of failure. More frequent inspections are required as the structure ages. Therefore, fracture mechanic analysis enables a more rational approach for writing those parts of specifications related to inspection.

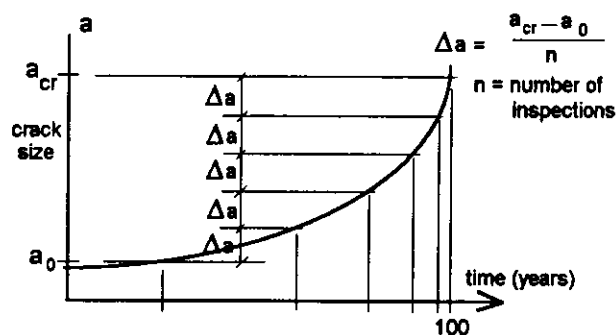


Figure 31 Crack growth curve

As the number of structures that approach or exceed their design life grows exponentially each year, so does the number of structures which have a high probability of containing fatigue cracks. Fracture mechanics will become an essential part of the assessment of these structures and, consequently, the decisions concerning their strengthening, repair and replacement. Cracking in several North American steel bridges was reviewed in a collection of case studies [26]. Finally, fracture mechanics analyses may assist in the assessment of complex structures that have connections which are not covered by test results. Test data obtained from simple beams and small specimens may be inapplicable to large structures and to

complex loading. This is particularly true for offshore structures, and some of these have been analyzed extensively using fracture mechanics.

References

1. I.F.C. Smith and M.A. Hirt, "Fracture Mechanics in Structural Engineering", *Steel Structures; Recent Research Advances and Their Application to Design*, M.N. Pavolic, Editor, Elsevier, 1986, Chapter VI, 381-402.
2. Griffith, A.A., "The Phenomena of Rupture and Flow in Solids", *Phil. Trans. Royal Soc. London (Series A)*, 221 (1921), 163-198.
3. Irwin, G.R., and de Wit, R., "A Summary of Fracture-Mechanics Concepts", *J. Testing Evaluation*, 11 (1983), 56-65.
4. Rolfe, S.T., "Fracture and Fatigue Control in Steel Structures", *Eng. J. Am. Inst. Steel Constr.*, 14 (1983), 2-15.
5. Smith, R.A., "An Introduction to Fracture Mechanics for Engineers – Parts I, II, and III", *Materials Eng. Applic.*, 1 (1978-79), 121-128, 227-235 and 316-322.
6. Broek, D., *Elementary Engineering Fracture Mechanics*, The Hague, Martinus Nijhoff, 1984.
7. Parker, A.P., *The Mechanics of Fracture and Fatigue*, London, Spon, 1981.
8. Rolfe, S.T. and Barsom, J.M., *Fracture and Fatigue Control in Structures*, 2nd Ed., Englewood Cliffs (New Jersey), Prentice-Hall, 1987.
9. Pellini, W.S., *Guidelines for Fracture-Safe and Fatigue-Reliable Design of Steel Structures*, Cambridge, Welding Inst., 1983.
10. Tada, H., Paris, P. and Irwin, G., *The Stress Analysis of Cracks Handbook*, St. Louis, Paris Productions, 1985.
11. Rooke, D.P. and Cartwright, D.J., *A Compendium of Stress Intensity Factors*, London, HMSO, 1976.
12. "J, a Measure of Fracture Toughness", in *ASTM E 813-81 (ASTM Book of Standards 3.01)* ASTM 1983, pp. 762-780.
13. Lankford, J., "The Influence of Microstructure on the Growth of Small Fatigue Cracks", *Fatigue Fracture Eng. Materials Struct.*, 8 (1985), 161-175.
14. Paris, P. and Erdogan, F., "A Critical Analysis of Crack Propagation Laws", *Trans. ASME (Series D)*, 85 (1963), 528-534.
15. European Convention for Constructional Steelwork, "Recommendations for the Fatigue Design of Steel Structures", ECCS Technical Committee 6, Rotterdam, 1985.

16. *Code of Practice for Fatigue (BS 5400: Part 10. Steel, Concrete and Composite Bridges)*, Brit. Standards Inst., 1980.
17. Suresh, S. and Richie, R.O. , "Propagation of Short Fatigue Cracks", *Int. Metals Rev.*, **29** (1984), 445-476.
18. Allen, R.J., "Quality Standards for Bridge Welds", in *Proceedings of the 2nd International Conference on Fatigue and Fatigue Thresholds (Fatigue 84)*, University of Birmingham, 1984, pp. 1729-1740.
19. Gurney, T.R., "Theoretical Analysis of the Influence of Attachment Size on the Fatigue Strength of Transverse Non-Load-Carrying Fillet Welds", *Members Rept. 91/1979*. Welding Inst. Cambridge, 1979.
20. Berge, S., "Effect of Plate Thickness in Fatigue of Cruciform Welded Joints", Rept. MK/R 67,. Norwegian Inst. Tech., Trondheim, 1983.
21. *Offshore Installation: Guidance on Design and Construction*, HMSO, 1984.
22. Smith, I.F.C. and Gurney, T.R., "Numerical Study of Geometrical Effects in Longitudinal Non-Load-Carrying Fillet-Welded Joints", *Welding Journal*, Vol.65, American Welding Society, Miami, 1985.
23. Gurney, T.R., *Fatigue of Welded Structures*, 2nd Edition, Cambridge University Press, 1979.
24. Fisher, J.W., Frank, K.H., Hirt, M.A., and McNamee, B.M., "Effect of Weldments on the Fatigue Strength of Steel Beams, National Cooperative Highway Research Program *Report 102*, Highway Research Board, Washington, D.C., 1970.
25. Fisher, J.W., Albrecht, P.A., Yen, B.T., Klingerman, D.J., and McNamee, B.M., "Fatigue Strength of Steel Beams With Transverse Stiffeners and Attachments", National Cooperative Highway Research Program, *Report 147*, Highway Research Board, Washington, D.C., 1974.
26. Fisher, J.W., *Fatigue and Fracture in Steel Bridges: Case Studies*, Wiley Interscience, 1984.
27. Broek, D., *The Practical Use of Fracture Mechanics*, Kluwer Academic Publishers, Dordrecht, The Netherlands, 1989.
28. American Association of State Highway and Transportation Officials, *Standard Specifications for Highway Bridges*, 4th Draft Edition, AASHTO, Washington, D.C., April, 1992.
29. Canadian Standards Association, CAN/CSA-S6-88, "Design of Highway Bridges", Rexdale, Ontario, 1988.

30. Ministry of Transportation, Province of Ontario, "Ontario Highway Bridge Design Code – III", Downsview, Canada, 1988.
31. Bardell, G.R., and Kulak, G.L., "Fatigue Strength Behaviour of Steel Beams with Welded Details", *Structural Engineering Report No. 72*, University of Alberta, September, 1978.
32. Bannantine, J.A., Comer, J.J., and Handrock, J.L., *Fundamentals of Metal Fatigue Analysis*, Prentice-Hall, Englewood Cliffs, (New Jersey), 1990.
33. Matsuishi, M. and Endo, T., "Fatigue of Metals Subject to Varying Stress" *Jap. Soc. Mech. Engng*, Fukoda, Japan, March 1968.
34. Smith I.F.C., Castiglioni, C.A. and Keating, P.B. "An Analysis of Fatigue Recommendations Considering New Data" *IABSE Periodica*, 13, International Association of Bridge and Structural Engineering, Zurich, 1989.
35. Fisher, J.W., Yen, B.T. and Wang D. "Fatigue of Bridge Structures – a Commentary and Guide for Design, Evaluation and Investigation Of Cracking" *ATLSS Report No 89-02*, 1989.
36. PD 6493 "Guidance on Some Methods for the Derivation of Acceptance Levels for Defects in Fusion Welded Joints, Welding Standards Committee, BSI, UK, 1991.
37. Commission of the European Communities, Eurocode No. 3, Design of Steel Structures, draft November 1990.
38. Fisher, J.W., Yen, B.T. and Wang D. "Fatigue Strength of Riveted Bridge Members", *Journal of Structural Engineering*, ASCE, Vol. 116, No.11, November, 1990.
39. Maddox, S.J., "Fatigue Strength of Welded Structures," Second Edition, Abington Publishing, Cambridge, U.K., 1991
40. Fisher, J.W., "Fatigue Cracking in Bridges from Out-of-Plane Displacements," *Canadian Journal of Civil Engineering*, Vol. 5, No. 4, December 1978
41. Cheng, J.J., "Design of Steel Beams with End Copes", *Journal of Constructional Steel Research*, Vol. 25, 1993